

Control of Nonholonomic Mechanical Systems Using Virtual Surfaces

Scott M. Kyle¹

2019/06/20

¹Graduate student, DEPARTMENT OF MATHEMATICS AND STATISTICS, QUEEN'S UNIVERSITY,
KINGSTON, ON K7L 3N6, CANADA
Email: 14jb82@queensu.ca

Abstract

In this report we study the modelling of simple mechanical systems evolving on trivial principal bundles, specifically *locomotion* systems with nonholonomic constraints.

We show how we can model motion via group actions on configuration manifolds and assess the relationship between the constraints (and constrained variables) and the variables that physically induce motion on the vehicle by studying principal bundles.

With knowledge of the controllability (using the Lie algebra rank condition) of this formulation of a constrained simple mechanical system, we proceed to outlining a methodology to design a universal control algorithm for constrained mechanical systems using the method of virtual surfaces (or potential functions).

Lastly, we design a set of virtual surfaces to make a rolling disk (arguably the simplest practical nonholonomic system) stabilise to a point, track a path, and avoid a sequence of obstacles in the plane.

Contents

1	Introduction	4
2	Simple mechanical systems	6
2.1	Forced simple mechanical system with constraints	6
2.2	Rigid body systems	7
2.2.1	Configuration	7
2.2.2	Matrix Lie group representation	8
2.2.3	Unconstrained rigid body transformations	10
2.3	Kinematic constraints	12
2.3.1	Concepts from differential geometry	12
2.3.2	Affine differential geometry	15
3	Constraints and connections on Lie groups	16
3.1	Lie algebras of Lie groups	16
3.2	Base spaces and principal bundles	18
3.2.1	Left actions of locomotion systems	18
3.2.2	Modelling constraints as connections	21
4	Equations of motion	23
4.1	Inertia tensor and kinetic energy metric	23
4.2	Forces	24
4.3	Euler–Lagrange equations	25
4.4	Constrained Euler-Lagrange equation	25
5	Rolling disk and two-wheel robot example	27
5.1	Configuration	27
5.1.1	Rolling disk	27
5.1.2	Two-wheeled robot	27
5.2	Kinematic constraints	27
5.2.1	Rolling disk	27
5.2.2	Two-wheeled robot	29
5.3	Constraints and connections on Lie groups	30
5.3.1	Rolling disk	30
5.3.2	Two-wheeled robot	31
5.3.3	Constraint Connection	33
5.4	Equations of motion	34
5.4.1	Rolling disk	34
5.4.2	Two-wheeled robot	36
6	Control design using virtual surfaces	39
6.1	The physical system	39
6.2	The virtual system	40
6.2.1	The virtual equations of motion	41
6.2.2	Determining the components of the virtual force	41

6.3	Controlling the rolling disk	42
6.3.1	Determining the components of the virtual force for the rolling disk	43
6.3.2	Forced equations of motion	43
6.4	Designing the virtual force	44
6.5	Designing practical surfaces	47
6.5.1	Point stabilisation	48
6.5.2	Path tracking	50
6.5.3	Obstacle avoidance	51
7	Conclusions and future work	53
7.1	Conclusions	53
7.2	Future work	54

Chapter 1

Introduction

In this report we study the modelling of simple mechanical systems evolving on trivial principal bundles. Using this representation, we show how a velocity constraint distribution is used to represent the constrained equations of motion of a simple mechanical system.

For *locomotion* systems, i.e., mobile robots, where position and orientation are the coordinates of importance, we show how we can model motion via group actions on configuration manifolds. The term locomotion refers to autonomous movement from point to point. Additionally, we assess the relationship between the constraints (and constrained variables) and the variables that physically induce motion on the vehicle by studying principal bundles.

We outline a methodology to design a universal control algorithm for constrained mechanical systems using the method of virtual surfaces.

Lastly, we design a set of virtual surfaces to make a rolling disk (arguably the simplest practical nonholonomic system) stabilise to a point, track a path, and avoid a sequence of obstacles in the plane.

The desired outcome is a framework to control of autonomous vehicles (which are nothing other than constrained nonholonomic systems) in dynamic environments using virtual surfaces in a geometric control setting. The goal is to design a universal control law that allows a vehicle to navigate from one configuration to another, while being able to re-route in real-time based on observed obstacles and other vehicles. If we can demonstrate the ability to use virtual surfaces to steer a vehicle in a desirable way, the final task is identifying surfaces that can be used in practice. What makes this approach attractive is that it is not imperative to have a physical path planned, nor is there a need to recalculate the overall path using some prescribed path planning algorithm (typically, these are computationally heavy). All we need is an *a priori* map of our route (or area) and we update this map based on sensed data. The underlying assumption is that we can reliably detect (and identify) these objects and ascertain their global position. While we do not investigate the practicality of sensing, we present this methodology to show what can we do with this information.

The motivation of this work stems from the methodology developed by Panagou, et al. (see [11], [12], [13]) who use *reference vector fields* for mobile robot control. While this work produced results in a kinematic setting, there was not much mathematical foundation for the design of the vector fields used to steer the vehicles.

The main approach in this report focusses on group actions on manifolds and principal fibre bundles for locomotion systems. A significant amount of work was done on these topics

in the 1990s by Murray and Kelly in [8] and [9], Bloch in [2], Cortes, et al. in [7]. Typical locomotion systems studied include the unicycle, the rolling disk, and the snakeboard.

The approach using group actions on manifolds lends itself nicely to deriving the momentum equations for a mechanical system, something we do not investigate in this report, but Bloch, et al. explore this in [17], and Bullo, et al. in [5].

Rossetter in [14] and Streubel in [15] used *artificial potential fields* for lane departure warning system control algorithms. We extend this method, and again, add a geometric framework.

Further, we acknowledge the work done using *barrier functions* and *control Lyapunov functions*, for example, by Ames et al. in [1] and Braun and Kellet in [4]. Simply stated (and similar to the intention of our virtual potential function), a barrier function is a continuous function whose value on a point increases to infinity as the point approaches the boundary of the feasible (or allowable) region of an optimization problem. As this method originates from the study of optimization, there is a natural progression into assessing the stability of such systems using Lyapunov methods.

We develop the geometric framework based on the work by Bullo and Lewis in [6], who outline everything from kinematics, distributions, constraints, Euler-Lagrange equations, group actions, principal fibre bundles, and controllability.

Finally, we acknowledge the work done by Ohsawa in [10], who assessed the fibre controllability of a Sphero robot, however, there is minimal discussion into practical control design.

Chapter 2

Simple mechanical systems

This report centres around *locomotion* systems, i.e., mobile robots, where position and orientation are the coordinates of importance. Using a planar rigid body with three degrees of freedom as a basis, we investigate the motion of other locomotion system that are also parameterized by coordinates (θ, x, y) , but have varying equations of motion due to different geometric configurations and/or coordinates that can be actuated. Throughout this report, we will layer details to add complexity to the simple vehicle that will capture dynamics inherent in *nonholonomic* systems.

2.1. Forced simple mechanical system with constraints

To understand where we are going, we introduce a forced simple mechanical system with constraints.

Definition 2.1.1 (Forced affine connection system). A C^∞ -simple mechanical system with constraints is the 5-tuple $(\mathbb{Q}, \mathbb{G}, V, F, \mathcal{D})$, where

- (i) \mathbb{Q} is a C^∞ -manifold (called the *configuration manifold*),
- (ii) \mathbb{G} is a C^∞ -Riemannian metric on \mathbb{Q} (called the *kinetic energy metric*),
- (iii) $V \in C^\infty(\mathbb{Q})$ is a function on \mathbb{Q} (called the *potential function*),
- (iv) $F: \mathbb{R} \times T\mathbb{Q} \rightarrow T^*\mathbb{Q}$ is a C^∞ -vector bundle map over $\text{id}_{\mathbb{Q}}$ (called the *Lagrangian force*),
and
- (v) \mathcal{D} is a C^∞ -linear velocity constraint (called the *distribution*). •

One of the main objectives of this report is to utilize the vector bundle map, F , as a tool for controlling the trajectories of the system. We visit this in section 6. The purpose of this section is to familiarize ourselves with rigid body kinematics to obtain a notion of the distribution, \mathcal{D} . Using the distribution, we can assess controllability of the system, cast the constraints as a connection on a principal bundle, and derive the associated constrained equations of motion.

2.2. Rigid body systems

The geometric approach to modelling mechanical systems relies heavily on the ability to describe the configuration of the rigid body. A rigid body is a (possibly uncountable) collection of particles whose position relative to one another is fixed. A measure theoretic interpretation of this is given below.

Definition 2.2.1 (Rigid body). A *rigid body* is a pair (\mathcal{B}, μ) where $\mathcal{B} \subset \mathbb{R}^3$ is compact, and μ is a finite Borel measure on \mathbb{R}^3 with support equal to \mathcal{B} called the *mass distribution* for the body. The *mass* of the body is

$$\mu(\mathcal{B}) = \int_{\mathcal{B}} d\mu.$$

To describe the location of a rigid body, it is necessary to define some spatial and body coordinate frames. Let $\Sigma_{spatial} = (O_{spatial}, \{\mathbf{s}_1, \mathbf{s}_2, \mathbf{s}_3\})$, where $O_{spatial} \in \mathbb{R}^3$ is the location of the origin represented in the basis $\{\mathbf{s}_1, \mathbf{s}_2, \mathbf{s}_3\}$. Without loss of generality, this can be thought of as the origin.

The body frame is described by $\Sigma_{body} = (O_{body}, \{\mathbf{b}_1, \mathbf{b}_2, \mathbf{b}_3\})$, where $O_{body} \in \mathbb{R}^3$ is the location of the origin of the body in the spatial frame. The body frame moves with the body, i.e., $\{\mathbf{b}_1, \mathbf{b}_2, \mathbf{b}_3\}$ describes the physical orientation of the body.

The position of the body is specified by $\mathbf{r} = O_{body} - O_{spatial} \in \mathbb{R}^3$.

Assuming the spatial and body bases are defined in a consistent way (like a right-handed coordinate system), the vectors in the each basis are related by

$$\mathbf{O}(n) = \{\mathbf{R} \in \mathbb{R}^{n \times n} : \mathbf{R}\mathbf{R}^T = \mathbf{I}_n\}, \mathbf{SO}(n) = \{\mathbf{R} \in \mathbf{O}(n) : \det \mathbf{R} = \pm 1\},$$

the set of orthogonal and special orthogonal matrices.

The matrix $\mathbf{R} \in \mathbf{SO}(n)$ relates the components in $\{\mathbf{s}_1, \mathbf{s}_2, \mathbf{s}_3\}$ to components in $\{\mathbf{b}_1, \mathbf{b}_2, \mathbf{b}_3\}$. The a -th column of \mathbf{R} are the components of \mathbf{b}_a , $a \in \{1, 2, 3\}$, relative to the basis $\{\mathbf{s}_1, \mathbf{s}_2, \mathbf{s}_3\}$.

2.2.1. Configuration

Definition 2.2.2 (Free Mechanical System). A *free mechanical system* is a collection of $N_b \in \mathbb{N}$ rigid bodies. The possible positions of all bodies are then described by the set

$$\mathbf{Q}_{\text{free}} = \underbrace{\mathbf{SO}(3) \times \mathbb{R}^3 \times \cdots \times \mathbf{SO}(3) \times \mathbb{R}^3}_{N_b}.$$

As illustrated in Figure 2.1, a planar rigid body (for a plane at height ρ) is defined by, $\mathbf{r} = (x, y, \rho) \in \mathbb{R}^3$, and

$$\mathbf{R} = \begin{bmatrix} \cos \theta & -\sin \theta & 0 \\ \sin \theta & \cos \theta & 0 \\ 0 & 0 & 1 \end{bmatrix} \in \mathbf{SO}(3), \quad (2.2.1)$$

meaning $\mathbf{Q}_{\text{free}} = \mathbf{SO}(3) \times \mathbb{R}^3$. However, since the body only moves in the plane, the actual

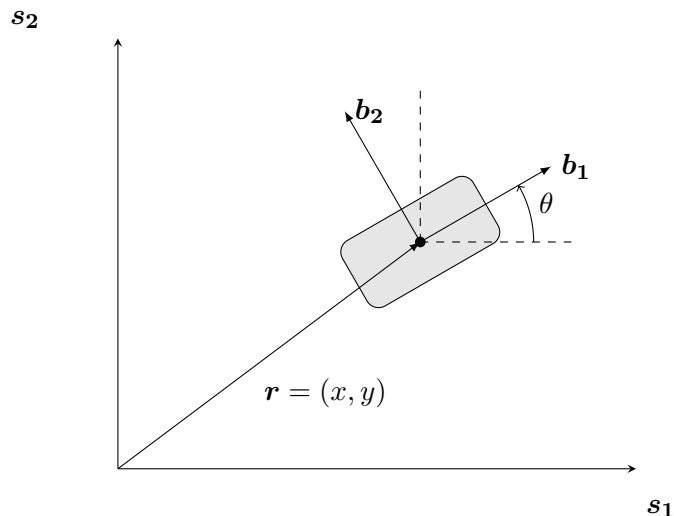


Figure 2.1: A planar rigid body

configuration of the body is the group $\mathbf{G} = \text{SO}(2) \times \mathbb{R}^2 = \text{SE}(2) \subset \mathbf{Q}_{\text{free}}$. The configuration manifold is parametrized by coordinates $g = (\theta, x, y)$.

We highlight the planar rigid body configuration as this forms a basis for the kinematic models of common locomotion systems. For example, when we want to “control” a rolling disk, two-wheeled mobile robot, or bicycle, we really want to move it to some (x, y) position, with orientation θ . That said, the specific kinematic model for each of these systems is different (and dependent on some *other* states and/or geometry), however we are able to characterise the *group* configuration in terms of *base* (or *shape*) variables. These base variables can often be thought of the variables that can be actuated. We explore this concept through two examples in Chapter 5: the rolling disk, and the two-wheeled differential drive robot.

2.2.2. Matrix Lie group representation

A matrix Lie group captures the position and orientation, i.e., the configuration, of the body as a rigid displacement matrix.

Definition 2.2.3 (Group). A set \mathbf{G} endowed with a binary operation denoted by $\mathbf{G} \times \mathbf{G} \ni (a, b) \mapsto a \star b$ is a *group* if:

- (i) $a \star (b \star c) = (a \star b) \star c$ for all $a, b, c \in \mathbf{G}$;
- (ii) there exists $e \in \mathbf{G}$ such that $a \star e = a$ for all $a \in \mathbf{G}$;
- (iii) there exists $a^{-1} \in \mathbf{G}$ such that $a \star a^{-1} = a^{-1} \star a = e$ for all $a \in \mathbf{G}$. •

Remark. The set $\text{GL}(n; \mathbb{R})$ of invertible $n \times n$ matrices with real entries is a *Lie group* with respect to the operation of matrix multiplication. It is called the *real general linear group*, or simply, the *general linear group*. The identity element is \mathbf{I}_n and the inverse element of $\mathbf{A} \in \text{GL}(n; \mathbb{R})$ is \mathbf{A}^{-1} . For all $n > 1$, the group is *non-Abelian* (non-commutative).

Definition 2.2.4 (Subgroup). Let G be a group.

- (i) A *subgroup* H of a group G is a subset of G such that $a \star (b \star c) = (a \star b) \star c$ for all $a, b, c \in G$.
- (ii) A *Lie subgroup* of Lie group G is subgroup of $H \subset G$ for which the inclusion $i_H: H \rightarrow G$ is an injective immersion (see Definition 2.3.1).
- (iii) A Lie subgroup H of G that is a submanifold of G is a *regular Lie subgroup*. •

Definition 2.2.5 (Matrix Lie group). A *matrix Lie group* is a Lie subgroup of $\text{GL}(n; \mathbb{R})$. •

To proceed, we need to introduce the concept of homogeneous coordinates. Let Σ_{spatial} and Σ_{body} be the spatial and body frames as in Definition 2.2.1, $\mathbf{r} \in \mathbb{R}^3$ and $\mathbf{R} \in \text{SO}(3)$.

The location of a point in space can be measured by an observer fixed either in the spatial or body frame. Let χ_s be the position of the body in the spatial frame and let χ_b be the position of the body in the body frame. The vectors are related by

$$\chi_s = \mathbf{R}\chi_b + \mathbf{r}. \quad (2.2.2)$$

For a vector $\mathbf{x} \in \mathbb{R}^n$, we define $\bar{\mathbf{x}} = (\mathbf{x}, 1) \in \mathbb{R}^{n+1}$ as the *homogeneous coordinates* of \mathbf{x} . With this definition, Equation (2.2.2) can be expressed as

$$\bar{\chi}_s = \begin{bmatrix} \mathbf{R} & \mathbf{r} \\ 0 & 1 \end{bmatrix} \bar{\chi}_b \quad (2.2.3)$$

and gives rise to Euclidean and special Euclidean groups as defined by

$$\begin{aligned} \mathbf{E}(n) &= \left\{ \mathbf{g} \in \mathbb{R}^{(n+1) \times (n+1)} : \mathbf{g} = \begin{bmatrix} \mathbf{R} & \mathbf{r} \\ 0 & 1 \end{bmatrix}, \mathbf{R} \in \text{O}(n), \mathbf{r} \in \mathbb{R}^n \right\}, \\ \mathbf{SE}(n) &= \{ \mathbf{g} \in \mathbf{E}(n) : \det \mathbf{g} = 1 \}. \end{aligned}$$

For the planar rigid body, where $n = 3$, the homogeneous coordinates are related by $\mathbf{g} \in \mathbf{SE}(3)$, given by the bijection

$$(\mathbf{R}, \mathbf{r}) \mapsto \begin{bmatrix} \mathbf{R} & \mathbf{r} \\ 0 & 1 \end{bmatrix}. \quad (2.2.4)$$

Example 2.2.1 (Planar Rigid Body). Let $\Sigma_{\text{spatial}} = ((0, 0, 0), \{\mathbf{s}_1, \mathbf{s}_2, \mathbf{s}_3\})$, where $\{\mathbf{s}_1, \mathbf{s}_2, \mathbf{s}_3\}$ is the standard basis for \mathbb{R}^3 . Let $\Sigma_{\text{body}} = ((x, y, \rho), \{\mathbf{b}_1, \mathbf{b}_2, \mathbf{b}_3\})$, where $\{\mathbf{b}_1, \mathbf{b}_2, \mathbf{b}_3\}$ is fixed in the body such that:

1. \mathbf{b}_1 is the body x -axis (and points in the instantaneous longitudinal direction of motion);
2. \mathbf{b}_2 is the body y -axis (and points in the instantaneous lateral direction of motion);
3. $\mathbf{b}_3 = \mathbf{s}_3$.

With $\mathbf{R} \in \text{SO}(3)$ as per Equation (2.2.1) and $\mathbf{r} = (x, y, \rho) \in \mathbb{R}^3$, we have that

$$\mathbf{g} = \begin{bmatrix} \cos \theta & -\sin \theta & 0 & x \\ \sin \theta & \cos \theta & 0 & y \\ 0 & 0 & 1 & \rho \\ 0 & 0 & 0 & 1 \end{bmatrix} \in \text{SE}(3), \quad (2.2.5)$$

and that, for a constant ρ , $g = (\theta, x, y) \in \mathbb{S}^1 \times \mathbb{R}^2$ is equivalent to $\mathbf{g} = (\mathbf{R}, \mathbf{r}) \in \text{SE}(3)$, and, under the group operation of matrix multiplication, is indeed a *group* as per Definition 3.1.4. The motion of the body in the plane is equivalent to a motion in $\text{SE}(3)$ (but can be reduced to a motion in $\text{SE}(2)$).

2.2.3. Unconstrained rigid body transformations

Rigid body motion is the combination of translations and rotations which are characterised by linear and angular velocities, respectively. In order to determine the rigid body's motion, we introduce some structure on the special Euclidean groups. This material is covered extensively in [6].

For $n \in \mathbb{N}$, let $\mathfrak{so}(n)$ be the vector space of skew-symmetric matrices in $\mathbb{R}^{n \times n}$ given by

$$\mathfrak{so}(n) = \{\mathbf{S} \in \mathbb{R}^{n \times n} : \mathbf{S}^T = -\mathbf{S}\}. \quad (2.2.6)$$

These skew-symmetric matrices represent the infinitesimal angular motion of the body. The physical spatial or body angular velocity can be extracted from these matrices using the *hat* map as defined below.

Let $\boldsymbol{\omega}, \boldsymbol{\alpha} \in \mathbb{R}^3$, and \times be the standard vector cross-product on \mathbb{R}^3 . The linear map $\hat{\cdot} : \mathbb{R}^3 \rightarrow \mathfrak{so}(3)$ is defined as $\hat{\boldsymbol{\omega}}\boldsymbol{\alpha} = \boldsymbol{\omega} \times \boldsymbol{\alpha}$. Thus, for $\boldsymbol{\omega} = (\omega^1, \omega^2, \omega^3)$,

$$\hat{\boldsymbol{\omega}} = \begin{bmatrix} 0 & -\omega^3 & \omega^2 \\ \omega^3 & 0 & -\omega^1 \\ -\omega^2 & \omega^1 & 0 \end{bmatrix}. \quad (2.2.7)$$

The inverse mapping $\check{\cdot} : \mathfrak{so}(3) \rightarrow \mathbb{R}^3$ is given by

$$\begin{bmatrix} 0 & -\omega^3 & \omega^2 \\ \omega^3 & 0 & -\omega^1 \\ -\omega^2 & \omega^1 & 0 \end{bmatrix}^{\check{\cdot}} = \boldsymbol{\omega}. \quad (2.2.8)$$

Similarly, let

$$\mathfrak{se}(n) = \left\{ \begin{bmatrix} \hat{\boldsymbol{\omega}} & \mathbf{v} \\ 0 & 0 \end{bmatrix} \in \mathbb{R}^{(n+1) \times (n+1)} : \hat{\boldsymbol{\omega}} \in \mathfrak{so}(n), \mathbf{v} \in \mathbb{R}^n \right\}.$$

Then the *hat* map, $\hat{\cdot}: \mathbb{R}^3 \oplus \mathbb{R}^3 \rightarrow \mathfrak{se}(3)$ for a given $\xi = (\omega, v) \in \mathbb{R}^3 \oplus \mathbb{R}^3$ is defined by

$$\hat{\xi} = \begin{bmatrix} \hat{\omega} & v \\ 0 & 0 \end{bmatrix}. \quad (2.2.9)$$

The vectors $\xi = (\omega, v) \in \mathbb{R}^3 \oplus \mathbb{R}^3$ are referred to as the *twist coordinates* (or simply *twists*), and represent velocity of the body in an inertial frame.

In the context of rigid body motion, the movement of a rigid body \mathcal{B} is described by a curve $t \mapsto \mathbf{g}(t) \in \text{SE}(3)$. We suppose the curve to be differentiable. The following two definitions apply given a curve $\mathbf{g}: \mathbb{R} \rightarrow \text{SE}(3)$.

Definition 2.2.6 (Body Velocity). The *body velocity* is the translational and angular velocities relative to the instantaneous body frame, and is defined by the curve $\xi_b: \mathbb{R} \rightarrow \mathbb{R}^3 \oplus \mathbb{R}^3$ given by $\hat{\xi}_b(t) = \mathbf{g}^{-1}(t)\dot{\mathbf{g}}(t)$. •

Definition 2.2.7 (Spatial Velocity). The *spatial velocity* is the translational and angular velocities relative to the spatial frame, and is defined by the curve $\xi_s: \mathbb{R} \rightarrow \mathbb{R}^3 \oplus \mathbb{R}^3$ given by $\hat{\xi}_s(t) = \dot{\mathbf{g}}(t)\mathbf{g}^{-1}(t)$. •

Example 2.2.2 (Planar Rigid Body). Continuing Example 2.2.1 and applying Definitions 2.2.6 and 2.2.7 gives

$$\begin{aligned} \hat{\xi}_b(t) &= \mathbf{g}^{-1}(t)\dot{\mathbf{g}}(t) \\ &= \begin{bmatrix} 0 & -\dot{\theta} & 0 & \dot{x} \cos \theta + \dot{y} \sin \theta \\ \dot{\theta} & 0 & 0 & -\dot{x} \sin \theta + \dot{y} \cos \theta \\ 0 & 0 & 0 & 0 \\ 0 & 0 & 0 & 0 \end{bmatrix}, \end{aligned} \quad (2.2.10)$$

$$\begin{aligned} \hat{\xi}_s(t) &= \dot{\mathbf{g}}(t)\mathbf{g}^{-1}(t) \\ &= \begin{bmatrix} 0 & -\dot{\theta} & 0 & \dot{x} + y\dot{\theta} \\ \dot{\theta} & 0 & 0 & \dot{y} - x\dot{\theta} \\ 0 & 0 & 0 & 0 \\ 0 & 0 & 0 & 0 \end{bmatrix}. \end{aligned} \quad (2.2.11)$$

Applying the *unhat* map gives the *twists*

$$\xi_b(t) = (\omega_b, v_b) = (\omega_b^x, \omega_b^y, \omega_b^z, v_b^x, v_b^y, v_b^z) = (0, 0, \dot{\theta}, \dot{x} \cos \theta + \dot{y} \sin \theta, -\dot{x} \sin \theta + \dot{y} \cos \theta, 0), \quad (2.2.12)$$

$$\xi_s(t) = (\omega_s, v_s) = (\omega_s^x, \omega_s^y, \omega_s^z, v_s^x, v_s^y, v_s^z) = (0, 0, \dot{\theta}, \dot{x} + y\dot{\theta}, \dot{y} - x\dot{\theta}, 0). \quad (2.2.13)$$

The relationship between the twist coordinates “equalling” some body velocity will become apparent when we introduce constraints and control inputs.

The reader is encouraged to think of these twists in the following way:

1. The body twist is the instantaneous velocity in the body frame, represented by the global configuration (θ, x, y) and associated velocities $(\dot{\theta}, \dot{x}, \dot{y})$. The body twist is the physical velocity of the body, and is used when calculating the kinetic energy of the motion.
2. The spatial twist should be thought of as the velocity of the body passing through $O_{spatial}$. It should be noted that the physical body might not be passing through the spatial origin. •

2.3. Kinematic constraints

Constraints arise naturally in simple mechanical systems due to the dependency of the instantaneous translational velocities on the orientation of the object and can be categorized into two categories, *holonomic* or *nonholonomic*.

At this point, we have not imposed any constraints on our planar rigid body, i.e., we assume the system is fully actuated and the body can travel instantaneously in its two translational coordinates (x, y) and its rotational coordinate θ . Discussions relating to controllability and control design are intuitive (and well known) in this instance.

The group configuration coordinates of the planar rigid body represent the coordinates of many interesting nonholonomic systems. The skate blade, unicycle, rolling disk and two-wheeled mobile robot fall into this category, however, we require some additional information to model and characterise the constraints of these systems.

Recall that $\xi_b = (\omega_b^x, \omega_b^y, \omega_b^z, v_b^x, v_b^y, v_b^z) = (0, 0, \dot{\theta}, \dot{x} \cos \theta + \dot{y} \sin \theta, -\dot{x} \sin \theta + \dot{y} \cos \theta, 0)$. The traditional skate blade model assumes there is a velocity, $u \in \mathbb{R}$, in the body x -axis, zero velocity in the body y -axis, and a turning rate $\omega \in \mathbb{R}$. With this assumption, Equation (2.2.12) reduces to $(\omega_b^z = \omega, v_b^x = u, v_b^y = 0) = (\dot{\theta}, \dot{x} \cos \theta + \dot{y} \sin \theta, -\dot{x} \sin \theta + \dot{y} \cos \theta)$.

This kinematic model is also used to for the unicycle, however, the drawback with this model and approach is that we cannot physically assign a translational velocity u . Since the constraint arises due to rolling, we must define u in terms of a rolling coordinate.

A rolling constraint occurs where the wheel is in contact with the ground. The velocity of the body at this point is identically zero. With an appropriate representation of the orientation of the body in $SE(n)$, the constraints are determined by

$$\begin{aligned} \bar{\chi}_s(t) = \mathbf{g}(t)\bar{\chi}_b(t) &\implies \frac{d}{dt}\bar{\chi}_s(t) = \frac{d}{dt}(\mathbf{g}(t)\bar{\chi}_b(t)) = \frac{d\mathbf{g}(t)}{dt}\bar{\chi}_b(t) + \mathbf{g}(t)\frac{d\bar{\chi}_b(t)}{dt} \\ &= \frac{d\mathbf{g}(t)}{dt}\mathbf{g}^{-1}(t)\bar{\chi}_s(t) = \hat{\xi}_s(t)\bar{\chi}_s(t) = \mathbf{0}. \end{aligned} \tag{2.3.1}$$

Therefore, we can use the spatial twist information to determine an expression for our velocity constraints.

2.3.1. Concepts from differential geometry

We introduce some concepts from differential geometry. We refer the reader to [6] for further details.

Let Q be a C^∞ -manifold of dimension n . We define T_qQ as the tangent space of Q at q and $v_q \in T_qQ$ as a tangent vector. Denote the total tangent bundle as $TQ = \bigcup_{q \in Q} T_qQ$.

If $f: Q \rightarrow V$ is a smooth mapping between C^∞ -manifolds, we write $T_qf: T_qQ \rightarrow T_{f(q)}V$ to denote the tangent map.

A vector field X on Q is a smooth mapping $X: Q \rightarrow TQ$, which assigns a tangent vector in T_qQ to each point q .

Definition 2.3.1 (Submersion and immersion). Let $f \in C^\infty(Q; V)$.

- (i) A *regular value* of f is a point $y \in V$ with the property that, for every $q \in f^{-1}(y)$, T_qf is surjective.
- (ii) For a subset $A \subset Q$, we say that f is a *submersion on A* if, for each $q \in A$, T_qf is surjective. If f is a submersion on Q , then it is simply a *submersion*.
- (iii) If T_qf is injective, we say f is an *immersion at q* . If f is an immersion at every $q \in Q$, we say that it is an *immersion*.

Distributions and codistributions

Determining the distribution of a constrained system is of utmost importance kinematically, as it captures what velocities are allowed at all points in the configuration space i.e., the vectors that form the tangent space (or a subspace of the tangent space). In fact, we will show that the most critical piece of information is the codistribution, as (mechanically speaking) this specifies the directions complementary to the directions we can move.

Definition 2.3.2 (Distributions and codistributions). Let Q be a C^∞ -manifold.

- (i) A *distribution* \mathcal{D} (resp. a *codistribution* Ω) is an assignment, to each point $q \in Q$, of a subspace \mathcal{D}_q of T_qQ (resp. a subspace Ω_q of T_q^*Q).
- (ii) A distribution (resp. codistribution) is C^∞ , if it is a C^∞ -generalized subbundle of TQ (resp. T^*Q).
- (iii) A C^∞ -distribution (resp. C^∞ -codistribution) is *regular* if it is a C^∞ -subbundle of TQ (resp. T^*Q). •

Definition 2.3.3 (Linear velocity constraint). Let Q be a C^∞ -differentiable manifold. A C^∞ -*linear velocity constraint* is a distribution on \mathcal{D} on Q with the property that $\text{ann}(\mathcal{D})$ is a C^∞ -codistribution. A C^∞ -linear velocity constraint \mathcal{D} is *regular* if \mathcal{D} is a regular distribution. A locally absolutely continuous curve $\gamma: [a, b] \rightarrow Q$ *satisfies* a constraint \mathcal{D} if $\gamma'(t) \in \mathcal{D}_{\gamma(t)}$ for a.e. $t \in [a, b]$. •

We refer the reader to [6] for detailed information on vector bundles and subbundles. Regularity of a distribution is equivalent to the distribution, \mathcal{D} , having locally constant rank. Assuming this condition holds, we have a C^∞ -distribution, which allows us to assess involutivity (and integrability), and therefore the holonomicity of the distribution.

Definition 2.3.4 (Involutive distribution). Let $r \in \mathbb{N} \cup \{\infty\} \cup \{\omega\}$. A C^∞ -distribution \mathcal{D} is *involutive* if, for every $q_0 \in \mathbb{Q}$ and for any pair of vector fields $X, Y \in \mathcal{D}$, it holds that $[X, Y] \in \mathcal{D}$, where $[\cdot, \cdot]$ is the Lie bracket. \bullet

Let \mathcal{D} be a C^∞ -distribution on a C^∞ -manifold \mathbb{Q} and let $q_0 \in \mathbb{Q}$. A *local integral manifold* through q_0 for \mathcal{D} is an immersed C^∞ -submanifold \mathbb{S} of a neighbourhood \mathcal{U} of q_0 with the property that, for each $q \in \mathbb{S}$, $\mathbb{T}_q \mathbb{S} \subset \mathcal{D}_q$. A local integral manifold \mathbb{S} is *maximal* if $\mathbb{T}_q \mathbb{S} = \mathcal{D}_q$ for each $q \in \mathbb{S}$. A maximal local integral manifold for \mathcal{D} containing $q \in \mathbb{Q}$ is the *maximal integral manifold* for \mathcal{D} through x if it contains any maximal local integral manifold through q . The distribution \mathcal{D} is *integrable* if there exists a maximal local integral manifold through each $q \in \mathbb{Q}$.

Under certain conditions and assumptions, there is a relationship between integrability and involutivity of a distribution.

Theorem 2.3.1 (Frobenius's Theorem). *The following statements hold:*

- (i) *a regular C^∞ -distribution is integrable if and only if it is involutive;*
- (ii) *a C^ω -distribution is integrable if and only if it is involutive.*

We refer the reader to [6] for the further detail.

Definition 2.3.5 (Holonomic and nonholonomic constraints). A regular linear velocity constraint \mathcal{D} is *holonomic* if \mathcal{D} is integrable. If a regular linear velocity constraint \mathcal{D} is not holonomic, it is *nonholonomic*. \bullet

As per [3], in our setting (and roughly speaking), nonholonomic constraints are velocity dependent, and are not derivable from position constraints. On the other hand, holonomic constraints are those that can be expressed in terms of position (and possibly time).

There are useful relationships between distributions and codistributions. In particular, given a distribution \mathcal{D} on \mathbb{Q} , we define the codistribution $\text{ann}(\mathcal{D})$ on \mathbb{Q} , called the *annihilator* of \mathcal{D} , by $(\text{ann}(\mathcal{D}))_q = \text{ann}(\mathcal{D}_q)$. Similarly, given a codistribution Ω on \mathbb{Q} , we define the distribution $\text{coann}(\Omega)$ on \mathbb{Q} , called the *coannihilator* of Ω , by $(\text{coann}(\Omega))_q = \text{coann}(\Omega_q)$.

Kinematic velocity constraints are used to determine the distribution on our configuration manifold. In coordinates, these constraints can be written in a general differential form as

$$\mathbb{T}_q^* \mathbb{Q} \ni \omega^j(q) = \alpha_i^j(q) dq^i, \quad i \in \{1, \dots, n\}, \quad j \in \{1, \dots, m\},$$

where n is the dimension of \mathbb{Q} , and m is the number of kinematic constraints.

Since covectors annihilate the vectors in the distribution, the image of the distribution is the kernel of the codistribution, i.e.,

$$\mathcal{D}_q = \text{span} \{X_i(q) \in \mathbb{T}_q \mathbb{Q} : \langle \omega^j(q), X_i(q) \rangle = 0 \quad \forall q \in \mathbb{Q}\}. \quad (2.3.2)$$

The local generators of \mathcal{D}_q^\perp are the vector fields $\mathbb{G}^\sharp(\omega^j(q)) \in \mathbb{T}_q \mathbb{Q}$ (the Riemannian metric \mathbb{G} is introduced in Section 4.1).

2.3.2. Affine differential geometry

Definition 2.3.6 (Affine connection). A C^∞ -affine connection on \mathbb{Q} assigns the pair $(X, Y) \in \Gamma^\infty(\mathbb{T}\mathbb{Q}) \times \Gamma^\infty(\mathbb{T}\mathbb{Q})$ a vector field $\nabla_X Y \in \Gamma^\infty(\mathbb{T}\mathbb{Q})$, and the assignment satisfies

- (i) the map $(X, Y) \mapsto \nabla_X Y$ is \mathbb{R} -bilinear,
- (ii) $\nabla_{fX} Y = f\nabla_X Y$ for each $X \in \Gamma^\infty(\mathbb{T}\mathbb{Q})$, $Y \in \Gamma^\infty(\mathbb{T}\mathbb{Q})$ and $f \in C^\infty(\mathbb{Q})$, and
- (iii) $\nabla_X fY = f\nabla_X Y + (\mathcal{L}_X f)Y$ for each $X \in \Gamma^\infty(\mathbb{T}\mathbb{Q})$, $Y \in \Gamma^\infty(\mathbb{T}\mathbb{Q})$ and $f \in C^\infty(\mathbb{Q})$.

The vector field $\nabla_X Y$ is called the *covariant derivative* of Y with respect to X . •

While we do not investigate the properties of affine connections or covariant derivatives in this report, we highlight the *Levi-Civita affine connection*, which is determined uniquely by the Riemannian metric \mathbb{G} . In coordinates, the geodesic equations are

$$\overset{\mathbb{G}}{\nabla}_{\gamma'(t)} \gamma'(t) = \left(\ddot{q}^i + \overset{\mathbb{G}}{\Gamma}_{jk}^i \dot{q}^j \dot{q}^k \right) \frac{\partial}{\partial q^i} = 0,$$

where $\overset{\mathbb{G}}{\Gamma}_{jk}^i: \mathbb{Q} \rightarrow \mathbb{R}$ are the *Christoffel symbols* of the *Levi-Civita affine connection*. The Christoffel symbols for $\overset{\mathbb{G}}{\nabla}$ are

$$\overset{\mathbb{G}}{\Gamma}_{ij}^k = \frac{1}{2} \overset{\mathbb{G}}{\Gamma}^{kl} \left(\frac{\partial \overset{\mathbb{G}}{\Gamma}_{il}}{\partial q^j} + \frac{\partial \overset{\mathbb{G}}{\Gamma}_{jl}}{\partial q^i} - \frac{\partial \overset{\mathbb{G}}{\Gamma}_{ij}}{\partial q^l} \right).$$

Chapter 3

Constraints and connections on Lie groups

There is an elegant way to characterise nonholonomic constraints on Lie groups. For most simple mechanical systems involving locomotion, we can exploit some inherent properties, most notably the rolling and spinning symmetry of wheels, and the fact we can generally actuate the rolling and spinning (steering) coordinates. The symmetry of the system allows us to reduce the dynamic system to a kinematic one, and assess the *kinematic controllability* of the system. While the theory can get complicated, it allows us to obtain some elegant results. For the next part of the report, we turn our attention to manifolds, group actions on manifolds, and principal fibre bundles.

Note, for the definitions in this section, we omit the bolded representation of a group element $\mathbf{g} \in \mathbf{G}$. We now write $g \in \mathbf{G}$.

3.1. Lie algebras of Lie groups

Sections 2.2.2 and 2.2.3 have identified a robust methodology to determine the velocity of a rigid body based on its configuration. The structure of special Euclidean groups $\mathbf{SE}(n)$ and the relationship with their associated *Lie algebras*, $\mathfrak{se}(n)$, is formalized with some theory of Lie algebras of Lie groups.

Definition 3.1.1 (Lie algebra). A *Lie algebra* \mathbf{V} is a \mathbb{R} -vector space endowed with a bilinear operation $[\cdot, \cdot] : \mathbf{V} \times \mathbf{V} \rightarrow \mathbf{V}$ called the *bracket* satisfying

- (i) anti-commutativity, i.e., $[\xi_1, \xi_2] = -[\xi_2, \xi_1]$ for all $\xi_1, \xi_2 \in \mathbf{V}$, and
- (ii) the Jacobi identity, i.e., $[\xi_1, [\xi_2, \xi_3]] + [\xi_2, [\xi_3, \xi_1]] + [\xi_3, [\xi_1, \xi_2]] = 0$ for all $\xi_1, \xi_2, \xi_3 \in \mathbf{V}$. •

Definition 3.1.2 (Left (resp. right) translation). For every $g \in \mathbf{G}$ the *left translation* (resp. *right translation*) by g is defined as the map $L_g : \mathbf{G} \rightarrow \mathbf{G}$ by $L_g(h) = g \star h$ for $h \in \mathbf{G}$ (resp. $R_g : \mathbf{G} \rightarrow \mathbf{G}$ by $R_g(h) = h \star g$). On Lie groups, the operation is matrix multiplication meaning $L_g(h) = gh$. •

The tangent map $\mathbb{T}_e L_g: \mathbb{T}_e \mathbb{G} \rightarrow \mathbb{T}_g \mathbb{G}$ is a natural isomorphism between $\mathbb{T}_e \mathbb{G}$ and $\mathbb{T}_g \mathbb{G}$, and as such we have an isomorphism between the tangent space and the tangent space at the identity.¹

One can easily verify that these tangent mappings represent the transformation from the vector representation of group velocities $v_g \in \mathbb{T}_g \mathbb{G}$ and the *unhat* expression of the group's body and spatial velocities (as given in Equations (2.2.12) and (2.2.13)), i.e., $v_g = \mathbb{T}_e L_g(\xi_b)$ and $v_g = \mathbb{T}_e R_g(\xi_s)$.

Definition 3.1.3 (Adjoint operator and adjoint mapping). Let \mathbb{G} be a Lie group with Lie algebra \mathfrak{g} and let $\xi, \eta \in \mathfrak{g}$. The *adjoint operator* is given by the linear map $\text{ad}_\eta: \mathfrak{g} \times \mathfrak{g}$ by

$$\text{ad}_\xi \eta = [\xi, \eta].$$

For $g \in \mathbb{G}$, the *adjoint mapping* $\text{Ad}_g: \mathfrak{g} \times \mathfrak{g}$ is given by

$$\text{Ad}_g = (\mathbb{T}_e R_g)^{-1} \circ \mathbb{T}_e L_g(\xi_b).$$

For $\xi, \eta \in \mathfrak{g}$, the adjoint maps satisfies the following property

$$\left. \frac{d}{dt} \right|_{t=0} \text{Ad}_{\exp(t\xi)}(\eta) = \text{ad}_\xi \eta.$$

Definition 3.1.4 (Lie algebra of a Lie group). The *Lie algebra* \mathfrak{g} of a Lie group \mathbb{G} is the tangent space at the identity $\mathbb{T}_e L_g$ with bracket $[\xi, \eta] = [\xi_L, \eta_L](e)$, where ξ_L, η_L are the vector fields defined by $g \mapsto \mathbb{T}_e L_g(\xi)$ and $g \mapsto \mathbb{T}_e L_g(\eta)$.

The motion of the body due to the motion of the base variables is described by the *left action* (resp. *right action*) of the base configuration \mathbb{G} on the total configuration \mathbb{Q} , defined below.

Definition 3.1.5 (Action of a group on a manifold). A *left action* (resp. *right action*) of a Lie group \mathbb{G} on a manifold \mathbb{Q} is a smooth map $\Phi: \mathbb{G} \times \mathbb{Q} \rightarrow \mathbb{Q}$ such that

(i) $\Phi(e, q) = q$ for all $q \in \mathbb{Q}$;

(ii) $\Phi(g_1, \Phi(g_2, q)) = \Phi(g_1 g_2, q)$ for every $g_1, g_2 \in \mathbb{G}$ and $q \in \mathbb{Q}$.

If $\Phi(g, q) = q$ implies $g = e$, then the left action is said to be *free*. If the map from $\mathbb{G} \times \mathbb{Q} \rightarrow \mathbb{Q} \times \mathbb{Q}$ defined by $(g, q) \mapsto (q, \Phi(g, q))$ is proper,² then the left action is said to be *proper*.

In simple mechanical systems, we take the manifold, \mathbb{Q} , to be the overall configuration of the system. One has some choice over the group and its action, however there are some intelligent and intuitive (but not unique) ways to choose the group and associated action. Since we are inducing motion by a group action, it seems natural to split the variables that vary by the group action, and the ones that do not, which leads to two submanifolds: the base (or shape) variables, \mathbb{M} , and the group variables, \mathbb{G} . To investigate this idea further, we define the base space and notion of a *trivial principal bundle*.

¹The identity e for $\text{SE}(n)$ is id^n , which implies $g = (\mathbf{R}, \mathbf{r}) = (\theta, x, y) = (0, 0, 0)$.

²A function $f: \mathbb{V} \rightarrow \mathbb{V}$ between two topological spaces is *proper* if $f^{-1}(\mathbb{K})$ is compact for every compact subset $\mathbb{K} \subset \mathbb{V}$.

3.2. Base spaces and principal bundles

Definition 3.2.1 (Base space). Let Q be a smooth manifold of dimension n , G be a group of dimension $n - m$ and suppose there exists a projection $\pi: Q \rightarrow Q/G$. The quotient space defined by $M = Q/G$ is the *base space* of our system and defines the internal configuration of the system. •

Definition 3.2.2 (Trivial principal bundle). A *trivial principal bundle* with base M and group G consists of the manifold $Q = M \times G$ together with a free left action of G on Q given by the left translation in the group variable: $\Phi_h(q) = \Phi_h(x, g) = \Phi(x, hg)$ for $x \in M$ and $g \in G$. •

There is an equivalent definition for right actions.

The manifold Q is called the *total space* of the bundle. For $x_0 \in M$, the set of points $(x_0, g) \in Q$ is called the *fibre over x_0* . In the trivial principal bundle case, $q = (x, g) \in M \times G$, and $v_q \in T_q Q$ can be written as $v_q = (v_x, v_g) \in T_x M \times T_g G$.

From now on, we denote a principal bundle as the 4-tuple (Q, M, G, π) .

There are many locomotion systems whose orientations are described by fibre configuration $g = (\theta, x, y)$. However, their total configurations are different due to base manifolds, M , that represent the variables that physically induce motion on the vehicle. Some examples include:

- (i) a spinning and rolling coordinate for the rolling disk (which can be reduced to a group configuration of (x, y));
- (ii) two rolling coordinates for a two-wheeled differential drive robot;
- (iii) or a rolling and steering coordinate for a kinematic car (or bicycle) model.

We explore the rolling disk and two-wheeled differential drive robot. We refer the reader to [8] for the kinematic car analysis.

3.2.1. Left actions of locomotion systems

Example 3.2.1 (Left action on a rolling disk). The rolling disk, of radius $\rho \in \mathbb{R}$, has a group configuration manifold $G = \mathbb{R}^2$, parameterized by coordinates (x, y) . A natural base space for the rolling disk is $M = \mathbb{S}^1 \times \mathbb{S}^1$, which represents the ability to apply input torques to spin and roll the disk about θ and ϕ respectively. The total configuration $Q = \mathbb{S}^1 \times \mathbb{S}^1 \times \mathbb{R}^2$ is depicted by Figure 3.1.

For an arbitrary $(s, t) \in \mathbb{R}^2$, the left action is

$$((s, t), (\phi, \theta, x, y)) \mapsto (\phi, \theta, x + s, y + t). \quad (3.2.1)$$

•

Example 3.2.2 (Left action on a two-wheeled robot). The two-wheeled robot, with wheels of radius $\rho \in \mathbb{R}$, has a group configuration manifold $G = SE(2)$ parametrized by coordinates θ, x, y . We are able to apply a torque to each wheel independently, giving $M = \mathbb{S}^1 \times \mathbb{S}^1$ with

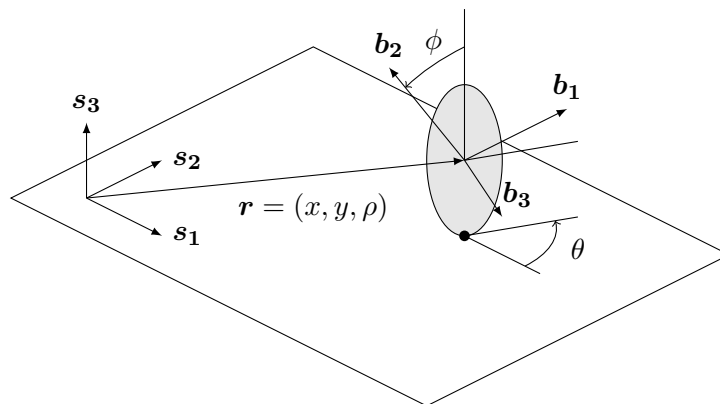


Figure 3.1: A rolling disk

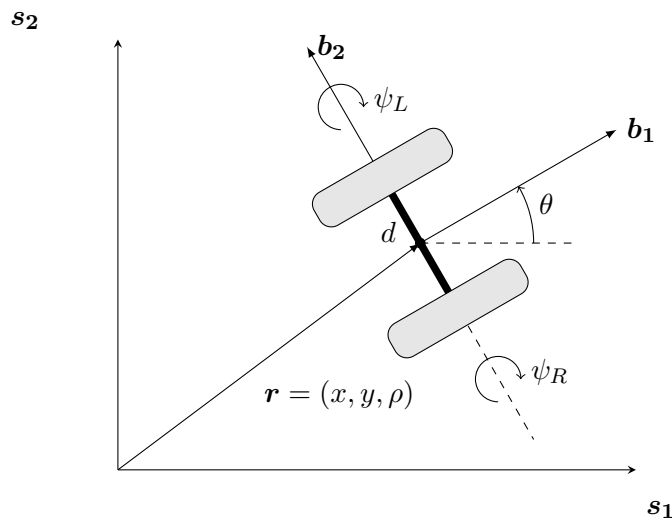


Figure 3.2: A two-wheel robot

coordinates (ψ_R, ψ_L) so that $\mathbf{Q} = \mathbb{S}^1 \times \mathbb{S}^1 \times \text{SE}(2)$. The total configuration is shown in Figure 3.2.

For an arbitrary $(\alpha, a, b) \in \text{SE}(2)$, the left action is

$$((\alpha, a, b), (\psi_R, \psi_L, \theta, x, y)) \mapsto (\psi_R, \psi_L, \theta + \alpha, x \cos \alpha - y \sin \alpha, x \sin \alpha + y \cos \alpha). \quad (3.2.2)$$

In Chapter 5, we determine the physical motion from the group actions above. We refer the reader to [2] and [8] for further details. •

Definition 3.2.3 (Group Orbits). Given a Lie group \mathbf{G} and a left action of \mathbf{G} on \mathbf{Q} , denoted by $\Phi_g(q)$, the *group orbit* through a point $q \in \mathbf{Q}$ is denoted

$$\text{Orb}(q) = \{\Phi_g(q) : g \in \mathbf{G}\}.$$

Definition 3.2.4 (Infinitesimal generators). Let Φ be a left action of M on a manifold Q , and $\xi \in \mathfrak{g}$ (the basis components of the Lie algebra). The *infinitesimal generator* of ξ is the vector field on Q defined by

$$\xi_Q(q) = \left. \frac{d}{d\epsilon} \Phi(\exp(\xi\epsilon), q) \right|_{\epsilon=0}. \quad (3.2.3)$$

Definition 3.2.5 (Tangent space to the group orbit). The *tangent space to the group orbit* through q is given by the set of *infinitesimal generators*, and denoted by

$$T_q(\text{Orb}(q)) = \{\xi_Q(q) : \xi \in \mathfrak{g}\}.$$

As per [7], if the action of G on Q is free and proper, the base (or quotient) space are the orbits of the system, and thus the projection map $\pi : Q \rightarrow Q/G$ is a smooth surjective map with a surjective tangent space $T_q\pi$ at each point, and is thus a trivial principal bundle. The kernel of the linear map $T_q\pi$ is the set of infinitesimal generators at the point q , i.e., it is exactly $T_q(\text{Orb}(q))$. This space is called the vertical subspace.

Definition 3.2.6 (Vertical subspace of principal fibre bundle). The *vertical subspace* of the principal fibre bundle Q at the point $q \in Q$ is

$$V_qQ = \{X \in T_qQ : X = \xi_Q(q) \text{ for } \xi \in \mathfrak{g}\}.$$

A vector which lies in V_qQ is tangent to the orbit of q under the action of G . For a trivial principal bundle $Q = M \times G$, the elements of V_qQ have the form $(0, \hat{\xi}_b g) \in T_qQ$ (where $\hat{\xi}_b \in \mathfrak{g}$ is body twist of the group variables). This follows from the fact the base variables are fully horizontal, and thus the vertical subspace is tangent to the fibre (group) variables.

Definition 3.2.7 (Connection on a principal bundle). A connection $\Gamma : TQ \rightarrow \mathfrak{g}$ (a \mathfrak{g} valued one form on Q) on the (trivial) principal bundle $Q = M \times G$ satisfies

- (i) $\Gamma(\xi_Q) = \xi$, and
- (ii) $\Gamma(T_q\Phi_g X) = \text{Ad}_g \Gamma(X)$.

Given $X \in T_qQ$, $\Gamma(X)$ is the unique $\xi \in \mathfrak{g}$ such that ξ_Q is equal to the vertical component of X .

A connection Γ on the principal fibre bundle Q assigns to each $q \in Q$ a horizontal subspace.

Definition 3.2.8 (Horizontal subspace of principal fibre bundle). The *horizontal subspace* of the principal fibre bundle \mathbb{Q} at the point $q \in \mathbb{Q}$ is

$$H_q\mathbb{Q} = \{X \in T_q\mathbb{Q} : \Gamma(X) = 0\}.$$

As per [8], it follows from the properties of the connection Γ that $T_q\mathbb{Q} = H_q\mathbb{Q} \oplus V_q\mathbb{Q}$ on a principal bundle. •

Since velocity vectors in the horizontal subspace are in the nullspace of the connection, one might wonder whether there is a relationship between the connection, Γ , and the codistribution, $\text{ann}(\mathcal{D})$. Indeed, there is the following relationship.

3.2.2. Modelling constraints as connections

Consider a system on a principal bundle $\mathbb{Q} = \mathbb{M} \times \mathbb{G}$ with constraints

$$\omega^j(q)v_q = 0, \quad j \in \{1, \dots, m\},$$

where $\omega^j(q) \in \text{ann}(\mathcal{D}_q)$. Let $\Gamma(q): T\mathbb{Q} \rightarrow \mathfrak{g}$ be the connection on the principal bundle. Let $\Phi_g: \mathbb{Q} \rightarrow \mathbb{Q}$ represent the left action of \mathbb{G} on \mathbb{Q} , and $\xi_{\mathbb{Q}}$ the infinitesimal generator associated with $\xi \in \mathfrak{g}$ (the Lie algebra of the group \mathbb{G}). The horizontal and vertical subspaces are:

- (i) $H_q\mathbb{Q} = \{X \in T_q\mathbb{Q} : \langle \omega^j(q); X \rangle = 0, \quad j \in \{1, \dots, m\}\},$
- (ii) $V_q\mathbb{Q} = \{\xi_{\mathbb{Q}}(q) \in T_q\mathbb{Q} : \xi \in \mathfrak{g}\}.$

If the constraints are group invariant, i.e., for any $g \in \mathbb{G}$ and $X \in T_q\mathbb{Q}$, we have $\Gamma(T_q\Phi_g(X)) = \text{Ad}_g\Gamma(X)$, and if $T_q\mathbb{Q} = V_q\mathbb{Q} \oplus H_q\mathbb{Q}$, the constraints define a distribution on $\mathbb{Q} = \mathbb{M} \times \mathbb{G}$. The constraints in terms of a connection one form are

$$\omega^j(q)v_q = 0 \iff \Gamma(q) \begin{bmatrix} v_x \\ v_g \end{bmatrix} = \text{Ad}_g(\xi + A(x)v_x) = 0, \quad (3.2.4)$$

where $A(x): T\mathbb{M} \rightarrow \mathfrak{g}$ is the *local representation* of the connection.

As per [7], Equation (3.2.4) is obtained by applying Definition 3.2.7, so that

$$\begin{aligned} \Gamma(q)v_q &= \Gamma(x, g)(v_x, v_g) = \Gamma(g(x, e))(g(v_x, \xi)) = \text{Ad}_g\Gamma(x, e)(v_x, \xi) \\ &= \text{Ad}_g(\Gamma(x, e)(0, \xi) + \Gamma(x, e)(v_x, 0)) \\ &= \text{Ad}_g(\xi + A(x)v_x). \end{aligned}$$

Similarly, splitting the constraints in terms of the trivial principal bundle and group coordinates (with normal coefficients), i.e., of the form

$$\omega^j(q) = dg^j + B_k^j(q)dx^k = 0, \quad j \in \{1, \dots, m\}, \quad k \in \{1, \dots, n - m\}, \quad B_k^j \in \mathbb{R},$$

with a matrix representation equivalent to $\Gamma(q)v_q = 0$, we get

$$\begin{aligned}
\Gamma(q)v_q = [\Gamma_x(q) \mid \Gamma_g(q)] \begin{bmatrix} v_x \\ v_g \end{bmatrix} &= \Gamma_g(q)v_g + \Gamma_x(q)v_x = 0 \\
\iff \mathbb{T}_e L_g \boldsymbol{\xi} + \Gamma_g^{-1}(q)\Gamma_x(q)v_x &= 0 \\
\iff \boldsymbol{\xi} + \underbrace{(\mathbb{T}_e L_g)^{-1}\Gamma_g^{-1}(q)\Gamma_x(q)}_{A(x)} v_x &= 0 \\
\iff \boldsymbol{\xi} + A(x)v_x &= 0 \\
\iff \text{Ad}_g(\boldsymbol{\xi} + A(x)v_x) &= 0.
\end{aligned}$$

Note that, the connection, Γ , is not unique.

Local controllability can be assessed using the one-form $A(x)$. In this report we use the Lie algebra rank condition to assess controllability, but we refer the reader to [8] for detail on fibre controllability. Also note, this expression determines the kinematic equations of motion since $\boldsymbol{\xi} = -A(x)v_x \implies \dot{g} = -gA(x)v_x$.

We now have a formal methodology for a trivial result. The main takeaway is that we have an expression for the motion of a locomotion system in terms of its base variables, i.e., the coordinates we can physically actuate.

Chapter 4

Equations of motion

We want to design a control framework based on the dynamics of the system, meaning we need to determine the equations of motion of a simple mechanical system. We will introduce the notions of inertia and kinetic energy; we refer the reader to [6] for a detailed overview of these ideas.

4.1. Inertia tensor and kinetic energy metric

We return to our discussion about an arbitrary rigid body, (\mathcal{B}, μ) . A rigid body is described by three properties: its mass, centre of mass, and inertia tensor, defined below.

Definition 4.1.1 (Centre of mass). The *centre of mass* of a body (\mathcal{B}, μ) is the point

$$\boldsymbol{\chi}_c = \frac{1}{\mu(\mathcal{B})} \left(\int_{\mathcal{B}} \boldsymbol{\chi} d\mu \right).$$

•

Definition 4.1.2 (Inertia tensor). Let (\mathcal{B}, μ) be a rigid body, and $\boldsymbol{\chi}_0$ its centre of mass. The *inertia tensor* about $\boldsymbol{\chi}_0$ of (\mathcal{B}, μ) is the linear map $\mathbb{I}_{\boldsymbol{\chi}_0} \in L(\mathbb{R}^3; \mathbb{R}^3)$ given by

$$\mathbb{I}_{\boldsymbol{\chi}_0}(\boldsymbol{v}) = \int_{\mathcal{B}} (\boldsymbol{\chi} - \boldsymbol{\chi}_0) \times (\boldsymbol{v} \times (\boldsymbol{\chi} - \boldsymbol{\chi}_0)) d\mu.$$

•

We denote the inertia tensor about the centre of mass of a rigid body (\mathcal{B}, μ) by \mathbb{I}_c .

The movement of the body \mathcal{B} is described by a curve $t \mapsto (\boldsymbol{r}(t), \boldsymbol{R}(t)) = \boldsymbol{g}(t) \in \text{SE}(3)$. As per Equation (2.2.2), a point $\boldsymbol{\chi}_b \in \mathcal{B}$ at time t is located at $\boldsymbol{\chi}_s(t) = \boldsymbol{R}(t)\boldsymbol{\chi}_b + \boldsymbol{r}(t)$.¹

Definition 4.1.3 (Kinetic energy). Let $\langle \cdot, \cdot \rangle_{\mathbb{R}^3}$ be the standard inner product on \mathbb{R}^3 , \boldsymbol{r} be the position of the body in the spatial frame, and $\boldsymbol{\omega}_b$ the body angular velocity (extracted

¹We use this fact, and a set of simplifying assumptions, to generalize the idea that the kinetic energy of a particle of mass m with velocity $\dot{\boldsymbol{x}}$, is $\frac{1}{2}m \|\dot{\boldsymbol{x}}\|^2$.

from the body twist coordinate). If the centre of mass is located at the origin of the body frame, the kinetic energy of (\mathcal{B}, μ) at time t is given by

$$KE(t) = \frac{1}{2}\mu(\mathcal{B}) \|\dot{\mathbf{r}}(t)\|_{\mathbb{R}^3}^2 + \frac{1}{2}\mathbb{G}_{\mathbb{R}^3}(\mathbb{I}_c(\boldsymbol{\omega}_b(t)), \boldsymbol{\omega}_b(t)).$$

If we parameterize our expression for kinetic energy in terms of velocities in the tangent bundle, instead of time, the kinetic energy metric is naturally a Riemannian metric on the configuration manifold. Let $(q^1, \dots, q^n) \in \mathcal{Q}$ be coordinates for our configuration manifold and $(v^1, \dots, v^n) \in \mathcal{T}\mathcal{Q}$, the associated tangent bundle. The Riemannian metric, \mathbb{G} , is defined as

$$\mathbb{G}_{ij} = \frac{\partial^2}{\partial v^i \partial v^j} KE.$$

Example 4.1.1 (Planar body kinetic energy). Let $\mu(\mathcal{B}) = m$ be the mass of the body and J the moment of inertia about the vertical axis,

$$KE = \frac{1}{2}m(\dot{x}(t)^2 + \dot{y}(t)^2) + \frac{1}{2}J\dot{\theta}(t)^2 = \frac{1}{2}m(v_x^2 + v_y^2) + \frac{1}{2}Jv_\theta^2.$$

Thus, the kinetic energy metric is

$$\mathbb{G} = m(dx \otimes dx + dy \otimes dy) + J(d\theta \otimes d\theta). \quad (4.1.1)$$

Referring back to Definition 2.1.1: we are now equipped with a configuration manifold \mathcal{Q} , a Riemannian metric \mathbb{G} on \mathcal{Q} , and a distribution \mathcal{D} .

Let us introduce F , a C^∞ -force.

4.2. Forces

Definition 4.2.1 (Forces). A C^∞ -force on $\mathcal{T}\mathcal{Q}$ is a map $F: \mathbb{R} \times \mathcal{T}\mathcal{Q} \rightarrow \mathcal{T}^*\mathcal{Q}$ with property that F is locally integrally class C^∞ bundle map over $\text{id}_{\mathcal{Q}}$. A C^∞ -force F is

- (i) *time-independent* if there exists a C^r -fibre bundle map $F_0: \mathcal{T}\mathcal{Q} \rightarrow \mathcal{T}^*\mathcal{Q}$ over $\text{id}_{\mathcal{Q}}$ with property that $F(t, v_q) = F_0(v_q)$, and is
- (ii) *basic* if there exists a C^∞ -covector field F_0 on \mathcal{Q} such that $F(t, v_q) = F_0(q)$.

If $\gamma: [a, b] \rightarrow \mathcal{Q}$ is a C^∞ -curve, then a C^∞ -force along γ is a C^∞ -covector field $F: [a, b] \rightarrow \mathcal{T}^*\mathcal{Q}$ along γ .

In coordinates, these forces can be written as a differential form as $F = F_i dq^i$, where F_i are called the *components* of the force F .

There are procedures in place to determine the *total external force* that acts on a rigid body. Due to the “simple” nature of our systems and forces (since they equate exactly to actuating the base variables), we do not explore this further.

4.3. Euler–Lagrange equations

We assume the reader is familiar with the calculus of variations and the Euler–Lagrange equations. For our discussion, we talk about the Euler–Lagrange equations on a Riemannian manifold. A time independent Lagrangian, $L: \mathbb{R} \rightarrow \mathbb{TQ}$, can be defined on this manifold as $L_{\mathbb{G}}(v_q) = \frac{1}{2}\mathbb{G}(v_q, v_q)$ —the kinetic energy of the system.

The geodesic equations $\overset{\mathbb{G}}{\nabla}_{\gamma'(t)}\gamma'(t) = 0$ are exactly the unforced equations of motions of a simple mechanical system.

Definition 4.3.1 (Forced Euler–Lagrange equations on Riemannian manifolds). Let (\mathbb{Q}, \mathbb{R}) be a C^∞ -Riemannian manifold, F a C^∞ -force, and $L_{\mathbb{G}}$ a C^∞ -Lagrangian. For a C^∞ -curve $\gamma: [a, b] \rightarrow \mathbb{Q}$, the *forced Euler–Lagrange equations* are

$$\overset{\mathbb{G}}{\nabla}_{\gamma'(t)}\gamma'(t) = \mathbb{G}^\sharp(F(t, \gamma'(t))). \quad (4.3.1)$$

•

4.4. Constrained Euler-Lagrange equation

Definition 4.4.1 (Orthogonal projections). Let \mathcal{D} be a regular C^∞ -linear velocity constraint on a C^∞ -manifold \mathbb{Q} . The *orthogonal projections* are C^∞ -vector bundle maps over $\text{id}_{\mathbb{Q}}$, denoted $P_{\mathcal{D}}, P_{\mathcal{D}}^\perp: \mathbb{TQ} \rightarrow \mathbb{TQ}$ such that, for each $v_q \in \mathbb{T}_q\mathbb{Q}$,

- (i) $v_q = P_{\mathcal{D}}(v_q) \oplus P_{\mathcal{D}}^\perp(v_q)$,
- (ii) $P_{\mathcal{D}}(v_q) \in \mathcal{D}_q$, and $P_{\mathcal{D}}^\perp(v_q) \in \mathcal{D}_q^\perp$,

where \mathcal{D}_q^\perp is the \mathbb{G} -orthogonal complement to \mathcal{D}_q , $P_{\mathcal{D}}$ is the \mathbb{G} -orthogonal projection onto \mathcal{D}_q , and $P_{\mathcal{D}}^\perp$ is the \mathbb{G} -orthogonal projection onto \mathcal{D}_q^\perp . •

These \mathbb{G} -orthogonal projections are calculated using the local representation of the distribution,

$$\mathcal{D}_q = \text{span} \{X_1, \dots, X_{n-m}: X_i \in \mathbb{T}_q\mathbb{Q}\},$$

and codistribution

$$\mathcal{D}_q^\perp = \text{span} \left\{ \mathbb{G}^\sharp(\omega^1), \dots, \mathbb{G}^\sharp(\omega^m): \omega^i \in \mathbb{T}_q^*\mathbb{Q} \right\}.$$

Definition 4.4.2 (Constrained forced Euler–Lagrange equations on Riemannian manifolds). Let (\mathbb{Q}, \mathbb{R}) be a C^∞ -Riemannian manifold, F a C^∞ -force, \mathcal{D} a regular C^∞ -linear velocity constraint, and $L_{\mathbb{G}}$ a C^∞ -Lagrangian. For a C^∞ -curve $\gamma: [a, b] \rightarrow \mathbb{Q}$, the *constrained forced Euler–Lagrange equations* are

$$\overset{\mathbb{G}}{\nabla}_{\gamma'(t)}\gamma'(t) = \mathbb{G}^\sharp(F(t, \gamma'(t))) + \lambda(t), \quad (4.4.1)$$

$$P_{\mathcal{D}}^\perp(\gamma'(t)) = 0, \quad (4.4.2)$$

where $\lambda(t) \in \mathcal{D}^\perp$, and $\gamma(t)$ is a controlled trajectory of the system.

The constraint force, $\lambda(t)$, is determined by differentiating Equation (4.4.2) along the trajectory, substituting in the dynamics of Equation (4.4.1) and solving, i.e.,

$$\begin{aligned}
P_{\mathcal{D}}^{\perp}(\gamma'(t)) = 0 &\implies \mathbb{G}_{\gamma'(t)}^{\mathbb{G}} \left(P_{\mathcal{D}}^{\perp}(\gamma'(t)) \right) = 0 \\
&\implies P_{\mathcal{D}}^{\perp} \left(\mathbb{G}_{\gamma'(t)}^{\mathbb{G}} \gamma'(t) \right) + \left(\mathbb{G}_{\gamma'(t)}^{\mathbb{G}} P_{\mathcal{D}}^{\perp} \right) (\gamma'(t)) = 0 \\
&\implies P_{\mathcal{D}}^{\perp} \left(\mathbb{G}^{\sharp}(F(t, \gamma'(t))) + \lambda(t) \right) + \left(\mathbb{G}_{\gamma'(t)}^{\mathbb{G}} P_{\mathcal{D}}^{\perp} \right) (\gamma'(t)) = 0 \\
&\implies \lambda(t) = -P_{\mathcal{D}}^{\perp} \left(\mathbb{G}^{\sharp}(F(t, \gamma'(t))) \right) - \left(\mathbb{G}_{\gamma'(t)}^{\mathbb{G}} P_{\mathcal{D}}^{\perp} \right) (\gamma'(t)). \tag{4.4.3}
\end{aligned}$$

Therefore, substituting (4.4.3) into (4.4.1) gives

$$\begin{aligned}
\mathbb{G}_{\gamma'(t)}^{\mathbb{G}} \gamma'(t) &= \mathbb{G}^{\sharp}(F(t, \gamma'(t))) - P_{\mathcal{D}}^{\perp} \left(\mathbb{G}^{\sharp}(F(t, \gamma'(t))) \right) - \left(\mathbb{G}_{\gamma'(t)}^{\mathbb{G}} P_{\mathcal{D}}^{\perp} \right) (\gamma'(t)) \\
\mathbb{G}_{\gamma'(t)}^{\mathbb{G}} \gamma'(t) &= P_{\mathcal{D}} \left(\mathbb{G}^{\sharp}(F(t, \gamma'(t))) \right) - \left(\mathbb{G}_{\gamma'(t)}^{\mathbb{G}} P_{\mathcal{D}}^{\perp} \right) (\gamma'(t)). \tag{4.4.4}
\end{aligned}$$

Chapter 5

Rolling disk and two-wheel robot example

5.1. Configuration

5.1.1. Rolling disk

The rolling disk is a rigid body with configuration manifold $Q = \mathbb{S}^1 \times \mathbb{S}^1 \times \mathbb{R}^2$, parameterised by coordinates $q = (\phi, \theta, x, y)$. The rolling coordinate is ϕ and the spinning coordinate is θ . A schematic of the rolling disk described in the following sections is given in figure 3.1. The total configuration of the rolling disk can be described by its orientation $\mathbf{R} \in \text{SO}(3)$ and position $\mathbf{r} = (x, y, \rho) \in \mathbb{R}^3$.

5.1.2. Two-wheeled robot

A two-wheeled differential drive robot is a rigid body with configuration manifold $Q = \mathbb{S}^1 \times \mathbb{S}^1 \times \text{SE}(2)$, parameterised by coordinates $q = (\psi_R, \psi_L, \theta, x, y)$. The coordinates ψ_R and ψ_L represent the rolling coordinates of the left and right wheel, which are separated by a distance $d \in \mathbb{R}_{>0}$. The two-wheel robot is kinematically related to the rolling disk as the forward velocity ($\rho\dot{\phi}$) and turning rate ($\dot{\theta}$) are uniquely determined by the combination of motion of each wheel. A schematic of the two-wheeled analysed in this section is given in figure 3.2.

5.2. Kinematic constraints

5.2.1. Rolling disk

Example 5.2.1 (Rolling disk constraints). The group representation of the disk is

$$\mathbf{g} = \begin{bmatrix} \cos \theta \cos \phi & \cos \theta \sin \phi & \sin \theta & x \\ \sin \theta \cos \phi & \sin \theta \sin \phi & -\cos \theta & y \\ -\sin \phi & \cos \phi & 0 & \rho \\ 0 & 0 & 0 & 1 \end{bmatrix} \in \text{SE}(3). \quad (5.2.1)$$

The spatial point of the disk that is in contact with the ground is directly down from the centre of mass. Therefore, the contact point is $\bar{\chi}_s = (x, y, 0, 1)$. Applying Equation (2.3.1) yields

$$\begin{aligned}
\bar{\chi}_s(t) &= \mathbf{g}(t)\bar{\chi}_b(t) \\
\frac{d}{dt}\bar{\chi}_s(t) &= \hat{\xi}_s(t)\bar{\chi}_s(t) \\
\mathbf{0} &= \begin{bmatrix} 0 & -\dot{\theta} & \dot{\phi} \cos \theta & \dot{x} + y\dot{\theta} - \rho\dot{\phi} \cos \theta \\ \dot{\theta} & 0 & \dot{\phi} \sin \theta & \dot{y} - x\dot{\theta} - \rho\dot{\phi} \sin \theta \\ -\dot{\phi} \cos \theta & -\dot{\phi} \sin \theta & 0 & \dot{\phi}(y \sin \theta + x \cos \theta) \\ 0 & 0 & 0 & 0 \end{bmatrix} \begin{bmatrix} x \\ y \\ 0 \\ 1 \end{bmatrix} \\
&= \begin{bmatrix} \dot{x} - \rho\dot{\phi} \cos \theta \\ \dot{y} - \rho\dot{\phi} \sin \theta \\ 0 \\ 0 \end{bmatrix} \implies \dot{x} = \rho\dot{\phi} \cos \theta, \dot{y} = \rho\dot{\phi} \sin \theta. \tag{5.2.2}
\end{aligned}$$

•

Example 5.2.2 (Rolling disk distribution). The constraints are local generators for $\text{ann}(\mathcal{D})$, expressed in differential form by

$$\omega^1(q) = dx - \rho \cos \theta d\phi = 0, \quad \omega^2(q) = dy - \rho \sin \theta d\phi = 0.$$

In matrix form, the constraints are

$$\underbrace{\begin{bmatrix} 1 & 0 & 0 & -\rho \cos \theta \\ 0 & 1 & 0 & -\rho \sin \theta \end{bmatrix}}_{\Omega(q)} \begin{bmatrix} \dot{x} \\ \dot{y} \\ \dot{\theta} \\ \dot{\phi} \end{bmatrix} = \begin{bmatrix} 0 \\ 0 \end{bmatrix}. \tag{5.2.3}$$

As per the definition, covectors annihilate the vectors in the distribution, meaning the image of the distribution is the kernel of the codistribution, $\Omega(q)$, i.e.,

$$\mathcal{D}_q = \text{span} \{X_i(q) \in \mathbb{T}_q\mathbb{Q} : \Omega(q)X_i(q) = 0 \forall q \in \mathbb{Q}\}. \tag{5.2.4}$$

A simple calculation shows that

$$\mathcal{D}_q = \text{span} \left\{ \begin{bmatrix} \rho \cos \theta \\ \rho \sin \theta \\ 0 \\ 1 \end{bmatrix}, \begin{bmatrix} 0 \\ 0 \\ 1 \\ 0 \end{bmatrix} \right\}, \tag{5.2.5}$$

which is well defined for all $q \in \mathbb{Q}$. The basis vectors (local generators) of \mathcal{D}_q in coordinates are

$$X_1 = \rho \cos \theta \frac{\partial}{\partial x} + \rho \sin \theta \frac{\partial}{\partial y} + \frac{\partial}{\partial \phi}, \quad X_2 = \frac{\partial}{\partial \theta}. \tag{5.2.6}$$

As per theorem 2.3.1, to check integrability of this distribution it suffices to check if the distribution is involutive. Start by computing

$$\begin{aligned} [X_1, X_2] &= -\rho \sin \theta \frac{\partial}{\partial x} + \rho \cos \theta \frac{\partial}{\partial y} \notin \mathcal{D}_q, \\ [X_2, [X_1, X_2]] &= \rho \cos \theta \frac{\partial}{\partial x} + \rho \sin \theta \frac{\partial}{\partial y} \notin \mathcal{D}_q. \end{aligned}$$

Higher order brackets can be shown to be in the span of previous brackets.

Clearly, the distribution is not involutive and, therefore, not integrable, which means the constraints are *nonholonomic*. We ascertain that the constraint is *totally nonholonomic* as the space spanned by $\{X_1, X_2, [X_1, X_2], [X_2, [X_1, X_2]]\}$ is linearly independent.

The four linearly independent Lie brackets imply kinematic controllability (more specifically small-time locally controllable) per the Lie algebra rank condition. We refer the reader to [6] for further detail. •

5.2.2. Two-wheeled robot

Example 5.2.3 (Two-wheeled robot constraints). The kinematic constraints of the two-wheeled robot are

$$\dot{x} = \frac{\rho}{2}(\dot{\psi}_R + \dot{\psi}_L) \cos \theta, \quad \dot{y} = \frac{\rho}{2}(\dot{\psi}_R + \dot{\psi}_L) \sin \theta, \quad \dot{\theta} = \frac{\rho}{d}(\dot{\psi}_R - \dot{\psi}_L). \quad (5.2.7)$$

Example 5.2.4 (Two-wheeled robot distribution). The constraints are local generators for $\text{ann}(\mathcal{D})$, expressed in differential form by

$$\begin{aligned} \omega^1(q) &= dx - \frac{\rho}{2} \cos \theta (d\psi_R + d\psi_L) = 0, \\ \omega^2(q) &= dy - \frac{\rho}{2} \sin \theta (d\psi_R + d\psi_L) = 0, \\ \omega^3(q) &= d\theta - \frac{\rho}{d} (d\psi_R - d\psi_L) = 0. \end{aligned}$$

In matrix form, the constraints are

$$\underbrace{\begin{bmatrix} 1 & 0 & 0 & -\frac{\rho}{2} \cos \theta & -\frac{\rho}{2} \cos \theta \\ 0 & 1 & 0 & -\frac{\rho}{2} \sin \theta & -\frac{\rho}{2} \sin \theta \\ 0 & 0 & 1 & -\frac{\rho}{d} & \frac{\rho}{d} \end{bmatrix}}_{\Omega(q)} \begin{bmatrix} \dot{x} \\ \dot{y} \\ \dot{\theta} \\ \dot{\psi}_R \\ \dot{\psi}_L \end{bmatrix} = \begin{bmatrix} 0 \\ 0 \\ 0 \end{bmatrix}. \quad (5.2.8)$$

Thus,

$$\mathcal{D}_q = \text{span} \left\{ \begin{bmatrix} \frac{\rho}{2} \cos \theta \\ \frac{\rho}{2} \sin \theta \\ \frac{\rho}{d} \\ 1 \\ 0 \end{bmatrix}, \begin{bmatrix} \frac{\rho}{2} \cos \theta \\ \frac{\rho}{2} \sin \theta \\ -\frac{\rho}{d} \\ 0 \\ 1 \end{bmatrix} \right\}, \quad (5.2.9)$$

which is well defined for all $q \in \mathbf{Q}$. The basis vectors (local generators) of \mathcal{D}_q in coordinates are

$$X_1 = \frac{\rho}{2} \cos \theta \frac{\partial}{\partial x} + \frac{\rho}{2} \sin \theta \frac{\partial}{\partial y} + \frac{\rho}{d} \frac{\partial}{\partial \theta} + \frac{\partial}{\partial \psi_R}, \quad X_2 = \frac{\rho}{2} \cos \theta \frac{\partial}{\partial x} + \frac{\rho}{2} \sin \theta \frac{\partial}{\partial y} - \frac{\rho}{d} \frac{\partial}{\partial \theta} + \frac{\partial}{\partial \psi_L}. \quad (5.2.10)$$

Again, one can check if the distribution is involutive. After this calculation we determine the system is not integrable which means the constraints are *nonholonomic*. We also ascertain that the space spanned by the Lie brackets imply has dimension of the configuration space, and is controllable per the Lie algebra rank condition. •

5.3. Constraints and connections on Lie groups

5.3.1. Rolling disk

Left actions

Example 5.3.1 (Left action on a rolling disk). The rolling disk, of radius $\rho \in \mathbb{R}$, has a group configuration manifold $\mathbf{G} = \mathbb{R}^2$, parameterized by coordinates (x, y) . A natural base space for the rolling disk is $\mathbf{M} = \mathbb{S}^1 \times \mathbb{S}^1$, which represent the ability to apply input torques to spin and roll the disk about θ and ϕ respectively. The total configuration $\mathbf{Q} = \mathbb{S}^1 \times \mathbb{S}^1 \times \mathbb{R}^2$. For an arbitrary $(s, t) \in \mathbb{R}^2$, the left action is

$$((s, t), (\phi, \theta, x, y)) \mapsto (\phi, \theta, x + s, y + t). \quad (5.3.1)$$

•

Tangent maps

(Note, we omit the bolded notation for group elements.)

Example 5.3.2 (Tangent maps for the rolling disk). Let $g = (x, y) \in \mathbf{G}$ and $h = (u, v) \in \mathbf{G}$. Let $L_g: \mathbf{G} \rightarrow \mathbf{G}$ by $L_g(h) = g \star h = gh = (x + u, y + v)$. Then

$$\begin{aligned} \mathbb{T}_e L_g &= \mathbb{T}_h L_g|_{h=e} = \left. \frac{\partial}{\partial h}(gh) \right|_{h=e} \\ &= \begin{bmatrix} 1 & 0 \\ 0 & 1 \end{bmatrix}. \end{aligned} \quad (5.3.2)$$

The calculation is similar for $R_g: \mathbf{G} \rightarrow \mathbf{G}$ defined by $R_g(h) = h \star g = hg = (u + x, v + y)$. •

Example 5.3.3 (Adjoint for the rolling disk). The matrix representation of the adjoint representation is

$$[\text{Ad}_g] = \begin{bmatrix} 1 & 0 \\ 0 & 1 \end{bmatrix}. \quad (5.3.3)$$

•

Example 5.3.4 (Infinitesimal generator for \mathbb{R}^2). Let $\mathbf{G} = \mathbb{R}^2$. Let $\Phi: \mathbf{G} \times \mathbf{Q} \rightarrow \mathbf{Q}$ be the standard left action of $\text{SE}(2)$ on itself. A standard basis of \mathfrak{g} , the Lie algebra of \mathbf{G} is

$$\xi_x = \begin{bmatrix} 1 \\ 0 \end{bmatrix} u, \quad \xi_y = \begin{bmatrix} 0 \\ 1 \end{bmatrix} v, \quad (5.3.4)$$

where $u, v \in \mathbb{R}$ are the local expressions for body velocity (in this case $u = \dot{x}$ and $v = \dot{y}$). Then,

$$\begin{aligned} \xi_{\mathbf{Q}}(q) &= \left. \frac{d}{d\epsilon} \Phi(\exp(\xi\epsilon), q) \right|_{\epsilon=0} = \left. \frac{d}{d\epsilon} \Phi(\exp(\xi\epsilon), g) \right|_{\epsilon=0} \\ &= \left. \frac{d}{d\epsilon} (\exp(\xi\epsilon)g) \right|_{\epsilon=0} \\ &= (\xi \exp(\xi\epsilon)g) \Big|_{\epsilon=0} \\ &= u \frac{\partial}{\partial x} + v \frac{\partial}{\partial y}. \end{aligned} \quad (5.3.5)$$

We know, for the left action described in Equation (5.3.1), the shape space is exactly $\mathbf{Q}/\mathbf{G} = \mathbf{M}$, and is thus a trivial principal bundle with infinitesimal generator

$$\xi_{\mathbf{Q}}(q) = \underbrace{0 \left(\frac{\partial}{\partial \phi} + \frac{\partial}{\partial \theta} \right)}_{\xi_{\mathbf{M}}(q)} + \underbrace{u \frac{\partial}{\partial x} + v \frac{\partial}{\partial y}}_{\xi_{\mathbf{G}}(q)}. \quad (5.3.6)$$

•

5.3.2. Two-wheeled robot

Left action

Example 5.3.5 (Left action on a two-wheeled robot). The two-wheeled robot, with wheels of radius $\rho \in \mathbb{R}$, has a group configuration manifold $\mathbf{G} = \text{SE}(2)$ parametrized by coordinates (θ, x, y) . We are able to apply a torque to each wheel independently, giving $\mathbf{M} = \mathbb{S}^1 \times \mathbb{S}^1$ with coordinates (ψ_R, ψ_L) so that $\mathbf{Q} = \mathbb{S}^1 \times \mathbb{S}^1 \times \text{SE}(2)$. For an arbitrary $(\alpha, a, b) \in \text{SE}(2)$, the left action is

$$((\alpha, a, b), (\psi_R, \psi_L, \theta, x, y)) \mapsto (\psi_R, \psi_L, \theta + \alpha, x \cos \alpha - y \sin \alpha + a, x \sin \alpha + y \cos \alpha + b). \quad (5.3.7)$$

•

Tangent maps

Example 5.3.6 (Tangent maps for the two-wheeled robot). Let $g = (\theta, x, y) \in \mathbf{G}$ and $h = (\beta, u, v) \in \mathbf{G}$. Let $L_g: \mathbf{G} \rightarrow \mathbf{G}$ by $L_g(h) = g \star h = gh = (\theta + \beta, u \cos \theta - v \sin \theta + x, u \sin \theta +$

$v \cos \theta + y$). Then

$$\begin{aligned}
\mathbb{T}_e L_g &= \mathbb{T}_h L_g|_{h=e} \\
&= \left. \frac{\partial}{\partial h}(gh) \right|_{h=e} \\
&= \left. \frac{\partial}{\partial h}(\theta + \beta, u \cos \theta - v \sin \theta + x, u \sin \theta + v \cos \theta + y) \right|_{h=e} \\
&= \begin{bmatrix} 1 & 0 & 0 \\ 0 & \cos \theta & -\sin \theta \\ 0 & \sin \theta & \cos \theta \end{bmatrix} \Big|_{h=e} = \begin{bmatrix} 1 & 0 & 0 \\ 0 & \cos \theta & -\sin \theta \\ 0 & \sin \theta & \cos \theta \end{bmatrix}. \tag{5.3.8}
\end{aligned}$$

Similarly, let $R_g: \mathbf{G} \rightarrow \mathbf{G}$ by $R_g(h) = h \star g = hg = (\beta + \theta, x \cos \beta - y \sin \beta + u, x \sin \beta + y \cos \beta + v)$. Then

$$\begin{aligned}
\mathbb{T}_e R_g &= \mathbb{T}_h R_g|_{h=e} \\
&= \left. \frac{\partial}{\partial h}(hg) \right|_{h=e} \\
&= \begin{bmatrix} 1 & 0 & 0 \\ -x \sin \beta - y \cos \beta & 1 & 0 \\ x \cos \beta - y \sin \beta & 0 & 1 \end{bmatrix} \Big|_{h=e} = \begin{bmatrix} 1 & 0 & 0 \\ -y & 1 & 0 \\ x & 0 & 1 \end{bmatrix}. \tag{5.3.9}
\end{aligned}$$

Example 5.3.7 (Adjoint for the two-wheeled robot). Using the tangent maps from Example 5.3.6, the matrix representation of the adjoint representation is

$$[\text{Ad}_g] = \begin{bmatrix} 1 & 0 & 0 \\ y & \cos \theta & -\sin \theta \\ -x & \sin \theta & \cos \theta \end{bmatrix}. \tag{5.3.10}$$

Example 5.3.8 (Infinitesimal generator for $\text{SE}(2)$). Let $\mathbf{G} = \text{SE}(2)$ and $\mathbf{Q} = \mathbf{G}$ and $g = (\mathbf{R}, \mathbf{r}) \in \mathbf{G} = \text{SE}(2)$. Let $\Phi: \mathbf{G} \times \mathbf{Q} \rightarrow \mathbf{Q}$ be the standard left action of $\text{SE}(2)$ on itself. A standard basis of $\mathfrak{se}(2)$, the Lie algebra of $\text{SE}(2)$ is

$$\boldsymbol{\xi}_\theta = \begin{bmatrix} 0 & -1 & 0 \\ 1 & 0 & 0 \\ 0 & 0 & 0 \end{bmatrix} \omega, \quad \boldsymbol{\xi}_x = \begin{bmatrix} 0 & 0 & 1 \\ 0 & 0 & 0 \\ 0 & 0 & 0 \end{bmatrix} u, \quad \boldsymbol{\xi}_y = \begin{bmatrix} 0 & 0 & 0 \\ 0 & 0 & 1 \\ 0 & 0 & 0 \end{bmatrix} v \implies \boldsymbol{\xi} = \begin{bmatrix} 0 & -\omega & u \\ \omega & 0 & v \\ 0 & 0 & 0 \end{bmatrix}, \tag{5.3.11}$$

where $u, v, \omega \in \mathbb{R}$ are the local expressions for body velocity (the physical expressions are calculated in Equation (2.2.12)). Then,

$$\begin{aligned}
\boldsymbol{\xi}_{\mathbf{Q}}(q) &= \left. \frac{d}{d\epsilon} \Phi(\exp(\boldsymbol{\xi}\epsilon), q) \right|_{\epsilon=0} = \left. \frac{d}{d\epsilon} \Phi(\exp(\boldsymbol{\xi}\epsilon), g) \right|_{\epsilon=0} \\
&= \left. \frac{d}{d\epsilon} (\exp(\boldsymbol{\xi}\epsilon) g) \right|_{\epsilon=0} \\
&= (\boldsymbol{\xi} \exp(\boldsymbol{\xi}\epsilon) g)|_{\epsilon=0} \\
&= \omega \frac{\partial}{\partial \theta} + (u - \omega y) \frac{\partial}{\partial x} + (v + \omega x) \frac{\partial}{\partial y}. \tag{5.3.12}
\end{aligned}$$

We know, for the left action two-wheeled robot described in Equation (5.3.7), the shape space is exactly $\mathbf{Q}/\mathbf{G} = \mathbf{M}$, and is a trivial principal bundle with infinitesimal generator

$$\xi_{\mathbf{Q}}(q) = 0 \underbrace{\left(\frac{\partial}{\partial \psi_R} + \frac{\partial}{\partial \psi_L} \right)}_{\xi_{\mathbf{M}}(q)} + \underbrace{\omega \frac{\partial}{\partial \theta} + (u - \omega y) \frac{\partial}{\partial x} + (v + \omega x) \frac{\partial}{\partial y}}_{\xi_{\mathbf{G}}(q)}. \quad (5.3.13)$$

We are now ready to cast the constraints as a connection. •

5.3.3. Constraint Connection

Rolling disk

Example 5.3.9 (Constrained connection for the rolling disk). Let $\mathbf{M} = \mathbb{S}^1 \times \mathbb{S}^1$ and $\mathbf{G} = \mathbb{R}^2$, so that $\mathbf{Q} = \mathbb{S}^1 \times \mathbb{S}^1 \times \mathbb{R}^2$. The left action for this principal bundle is given by Equation (5.3.1), and associated infinitesimal generator (5.3.5).

The constraints, relating the base and group variables, are given in Equation (5.2.3).

Using this information, we get an expression for Γ that satisfies condition (i) of Definition 3.2.7. A calculation, by inspection, shows

$$\Gamma(\xi_{\mathbf{Q}}) = \xi \iff [\Gamma_x \mid \Gamma_g] \begin{bmatrix} \mathbf{0} \\ \xi_{\mathbf{G}} \end{bmatrix} = \xi \iff \Gamma_g(\xi_{\mathbf{G}}) = \xi \iff \Gamma_g = \mathbb{T}_e R_g^{-1}.$$

We can calculate the Γ_x knowing Γ must satisfy condition (i) in Definition 3.2.2, i.e., $\Gamma(X) = 0$, when $X \in \mathbf{H}_q \mathbf{Q}$, as

$$\begin{aligned} [\Gamma_x \mid \mathbb{T}_e R_g^{-1}](X) = 0 &\iff \Gamma_x(X_x) + \mathbb{T}_e R_g^{-1}(X_g) = 0 \\ \iff \Gamma_x \begin{bmatrix} 1 \\ 0 \end{bmatrix} + \mathbb{T}_e R_g^{-1} \begin{bmatrix} \rho \cos \theta \\ \rho \sin \theta \end{bmatrix} = 0, \Gamma_x \begin{bmatrix} 0 \\ 1 \end{bmatrix} + \mathbb{T}_e R_g^{-1} \begin{bmatrix} 0 \\ 0 \end{bmatrix} = 0 \\ \iff \Gamma_x = \begin{bmatrix} -\rho \cos \theta & 0 \\ -\rho \sin \theta & 0 \end{bmatrix} \\ \implies \Gamma = \begin{bmatrix} -\rho \cos \theta & 0 & 1 & 0 \\ -\rho \sin \theta & 0 & 0 & 1 \end{bmatrix}. \end{aligned}$$

We must now check condition (ii) of Definition 3.2.7.

$$\begin{aligned} \text{Ad}_g \Gamma(X) &= \begin{bmatrix} 1 & 0 \\ 0 & 1 \end{bmatrix} \begin{bmatrix} -\rho \cos \theta & 0 & 1 & 0 \\ -\rho \sin \theta & 0 & 0 & 1 \end{bmatrix} (X) \\ &= \Gamma(X). \\ \Gamma(\mathbb{T}_q \Phi_g(X)) &= \begin{bmatrix} -\rho \cos \theta & 0 & 1 & 0 \\ -\rho \sin \theta & 0 & 0 & 1 \end{bmatrix} \begin{bmatrix} 1 & 0 & 0 & 0 \\ 0 & 1 & 0 & 0 \\ 0 & 0 & 1 & 0 \\ 0 & 0 & 0 & 1 \end{bmatrix} (X) \\ &= \Gamma(X) = \text{Ad}_g \Gamma(X). \end{aligned}$$

Thus, we have met all the conditions of the connection one form, and the principal bundle is indeed a principal bundle. The local connection is, therefore,

$$A(x) = (\mathbb{T}_e L_g)^{-1} \Gamma_g^{-1}(q) \Gamma_x(q) = (\mathbb{T}_e L_g)^{-1} \mathbb{T}_e R_g \Gamma_x(q) = (\text{Ad}_g)^{-1} \Gamma_x(q) = \begin{bmatrix} -\rho \cos \theta & 0 \\ -\rho \sin \theta & 0 \end{bmatrix}.$$

Since $\xi = -A(x)v_x$, we deduce an expression for the group variables as

$$v_g = \mathbb{T}_e L_g \xi = -\mathbb{T}_e L_g A(x) v_x = \begin{bmatrix} \rho \cos \theta & 0 \\ \rho \sin \theta & 0 \end{bmatrix} \begin{bmatrix} \dot{\phi} \\ \dot{\theta} \end{bmatrix} = X_i^v u^i, \quad (5.3.14)$$

where $X_i^v \in \mathbb{T}_g \mathbb{G}$ are the vertical vector fields, and the control inputs $u^i = \dot{x}^i \in \mathbb{T}_x \mathbb{M}$. Since, $\mathbb{T}_q \mathbb{Q} = \mathbb{T}_x \mathbb{M} \oplus \mathbb{T}_g \mathbb{G}$, we can append the motion of the horizontal coordinates in the principal bundle, i.e., $\dot{\phi} = \dot{\phi}$ and $\dot{\theta} = \dot{\theta}$ to obtain the familiar distribution (and kinematic equation of motion) for the rolling disk, as given in Equation (5.2.6). •

Two-wheeled robot

Example 5.3.10 (Constrained connection for the two-wheeled robot). Let $\mathbb{M} = \mathbb{S}^1 \times \mathbb{S}^1$ and $\mathbb{G} = \text{SE}(2)$, so that $\mathbb{Q} = \mathbb{S}^1 \times \mathbb{S}^1 \times \text{SE}(2)$. The left action for this principal bundle is given by Equation (5.3.7), and associated infinitesimal generator (5.3.13).

The constraints, relating the base and group variables, are given in Equation (5.2.8).

The calculations are the same as Example 5.3.9, so we simply state the results. We get

$$\begin{aligned} \Gamma_g &= \mathbb{T}_e R_g^{-1}, \\ \Gamma_x &= \begin{bmatrix} -\frac{\rho}{d} & \frac{\rho}{d} \\ -\frac{\rho}{d} y - \frac{\rho}{2} \cos \theta & \frac{\rho}{d} y - \frac{\rho}{2} \cos \theta \\ \frac{\rho}{d} x - \frac{\rho}{2} \sin \theta & -\frac{\rho}{d} x - \frac{\rho}{2} \sin \theta \end{bmatrix}, \\ \Gamma &= \begin{bmatrix} -\frac{\rho}{d} & \frac{\rho}{d} & 1 & 0 & 0 \\ -\frac{\rho}{d} y - \frac{\rho}{2} \cos \theta & \frac{\rho}{d} y - \frac{\rho}{2} \cos \theta & y & 1 & 0 \\ \frac{\rho}{d} x - \frac{\rho}{2} \sin \theta & -\frac{\rho}{d} x - \frac{\rho}{2} \sin \theta & -x & 0 & 1 \end{bmatrix}, \\ A(x) &= \begin{bmatrix} -\frac{\rho}{d} & \frac{\rho}{d} \\ -\frac{\rho}{2} & -\frac{\rho}{2} \\ 0 & 0 \end{bmatrix}, \\ v_g &= \begin{bmatrix} \frac{\rho}{d} & -\frac{\rho}{d} \\ \frac{\rho}{2} \cos \theta & \frac{\rho}{2} \cos \theta \\ \frac{\rho}{2} \sin \theta & \frac{\rho}{2} \sin \theta \end{bmatrix} \begin{bmatrix} \dot{\psi}_R \\ \dot{\psi}_L \end{bmatrix} = X_i^v u^i, \end{aligned}$$

where $X_i^v \in \mathbb{T}_g \mathbb{G}$ are the vertical vector fields, and the control inputs $u^i = \dot{x}^i \in \mathbb{T}_x \mathbb{M}$. Again, we can append the motion of the horizontal coordinates in the principal bundle, i.e., $\dot{\psi}_R = \dot{\psi}_R$ and $\dot{\psi}_L = \dot{\psi}_L$ to obtain the same expression as given in Equation (5.2.10). •

5.4. Equations of motion

5.4.1. Rolling disk

Example 5.4.1 (Rolling disk kinetic energy). Let $\mu(\mathcal{B}) = m$ be the mass of the body, J_{spin} the moment of inertia about the vertical axis, and J_{roll} the moment of inertia

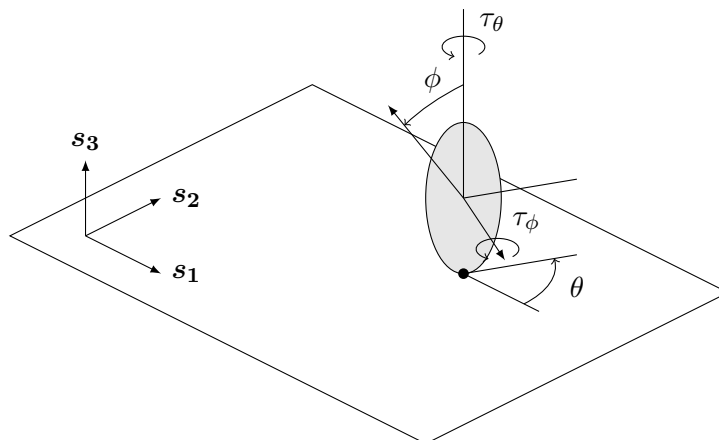


Figure 5.1: Forces on the rolling disk.

about the rolling axis, then calculate

$$KE = \frac{1}{2}m(\dot{x}^2 + \dot{y}^2) + \frac{1}{2}J_{spin}\dot{\theta}^2 + \frac{1}{2}J_{roll}\dot{\phi}^2.$$

The kinetic energy metric is, therefore,

$$\mathbb{G} = m(dx \otimes dx + dy \otimes dy) + J_{spin}(d\theta \otimes d\theta) + J_{roll}(d\phi \otimes d\phi). \quad (5.4.1)$$

•

Example 5.4.2 (Rolling disk forces). As per Figure 5.1, the forces acting on the rolling disk are torques represented by

$$F^1 = \tau_\theta(0, 0, 1, 0) = \tau_\theta d\theta, \quad F^2 = \tau_\phi(0, 0, 0, 1) = \tau_\phi d\phi,$$

with τ_θ and τ_ϕ defined on $\mathbb{R} \times \mathbb{TQ}$.

•

Example 5.4.3 (Rolling disk orthogonal projections). From Example 5.2.2 we have a basis for \mathcal{D}_q and \mathcal{D}_q^\perp . In matrix form, the bases are¹

$$G(q) = \begin{bmatrix} \rho \cos \theta & 0 \\ \rho \sin \theta & 0 \\ 0 & 1 \\ 1 & 0 \end{bmatrix}, \quad \Omega^T(q) = \begin{bmatrix} 1 & 0 \\ 0 & 1 \\ 0 & 0 \\ -\rho \cos \theta & -\rho \sin \theta \end{bmatrix}.$$

In Example 5.4.1, we calculated the Riemannian metric, which is given by

$$[\mathbb{G}] = \begin{bmatrix} m & 0 & 0 & 0 \\ 0 & m & 0 & 0 \\ 0 & 0 & J_{spin} & 0 \\ 0 & 0 & 0 & J_{roll} \end{bmatrix}.$$

¹We revert to the notation of our configuration being $q = (x, y, \theta, \phi)$ as opposed to the manifold and group order of $q = (\phi, \theta, x, y)$ as in previous sections.

Using the formula for the orthogonal projection (there are multiple ways to do this)

$$[P_{\mathcal{D}}] = G(q) (G(q)^T [\mathbb{G}] G(q))^{-1} G(q)^T [\mathbb{G}], \quad (5.4.2)$$

$$\begin{aligned} [P_{\mathcal{D}}^{\perp}] &= [\mathbb{G}]^{-1} \Omega^T(q) \left([\mathbb{G}]^{-1} \Omega(q) [\mathbb{G}] [\mathbb{G}]^{-1} \Omega^T(q) \right)^{-1} [\mathbb{G}]^{-1} \Omega(q) [\mathbb{G}] \\ &= [\mathbb{G}]^{-1} \Omega^T(q) \left([\mathbb{G}]^{-1} \Omega(q) \Omega^T(q) \right)^{-1} [\mathbb{G}]^{-1} \Omega(q) [\mathbb{G}], \end{aligned} \quad (5.4.3)$$

and we obtain

$$[P_{\mathcal{D}}] = \frac{1}{m\rho^2 + J_{roll}} \begin{bmatrix} m\rho^2 \cos^2 \theta & m\rho^2 \cos \theta \sin \theta & 0 & \rho J_{roll} \cos \theta \\ m\rho^2 \cos \theta \sin \theta & m\rho^2 \sin^2 \theta & 0 & \rho J_{roll} \sin \theta \\ 0 & 0 & 1 & 0 \\ m\rho \cos \theta & m\rho \sin \theta & 0 & J_{roll} \end{bmatrix}, \quad (5.4.4)$$

$$[P_{\mathcal{D}}^{\perp}] = \frac{1}{m\rho^2 + J_{roll}} \begin{bmatrix} J_{roll} + m\rho^2 \sin^2 \theta & -m\rho^2 \cos \theta \sin \theta & 0 & -\rho J_{roll} \cos \theta \\ -m\rho^2 \cos \theta \sin \theta & J_{roll} + m\rho^2 \cos^2 \theta & 0 & -\rho J_{roll} \sin \theta \\ 0 & 0 & 0 & 0 \\ -m\rho \cos \theta & -m\rho \sin \theta & 0 & m\rho^2 \end{bmatrix}. \quad (5.4.5)$$

•

Example 5.4.4 (Rolling disk equations of motion). Recall our expressions for \mathbb{G} , $P_{\mathcal{D}}$, $P_{\mathcal{D}}^{\perp}$, F^1 , F^2 , and let $\lambda^1, \lambda^2 \in \mathbb{R}$. The local representation of the equations of motion are

$$\begin{aligned} \ddot{x} &= \frac{1}{m} \lambda^1, \quad \ddot{y} = \frac{1}{m} \lambda^2, \quad \ddot{\theta} = \frac{1}{J_{spin}} \tau_{\theta}, \quad \ddot{\phi} = \frac{1}{J_{roll}} \tau_{\phi} - \lambda^1 \frac{\rho}{J_{roll}} \cos \theta - \lambda^2 \frac{\rho}{J_{roll}} \sin \theta, \\ \dot{x} &= \rho \dot{\phi} \cos \theta, \quad \dot{y} = \rho \dot{\phi} \sin \theta \end{aligned}$$

Solving for $\lambda^1, \lambda^2 \in \mathbb{R}$, i.e, the local representation of Equation (4.4.4), gives

$$\begin{aligned} \ddot{x} &= \frac{\rho \cos \theta}{m\rho^2 + J_{roll}} \tau_{\phi} - \rho \dot{\theta} \dot{\phi} \sin \theta, \quad \ddot{y} = \frac{\rho \sin \theta}{m\rho^2 + J_{roll}} \tau_{\phi} + \rho \dot{\theta} \dot{\phi} \cos \theta, \\ \ddot{\theta} &= \frac{1}{J_{spin}} \tau_{\theta}, \quad \ddot{\phi} = \frac{1}{m\rho^2 + J_{roll}} \tau_{\phi}. \end{aligned} \quad (5.4.6)$$

•

5.4.2. Two-wheeled robot

Example 5.4.5 (Two-wheeled robot kinetic energy). Let $\mu(\mathcal{B}) = m$ be the mass of the body, I_{body} the moment of inertia about the centre of mass, and J_{roll} the moment of inertia about the rolling axis of each wheel. We have

$$KE = \frac{1}{2} m (\dot{x}^2 + \dot{y}^2) + \frac{1}{2} I_{body} \dot{\theta}^2 + \frac{1}{2} J_{roll} (\dot{\psi}_R^2 + \dot{\psi}_L^2).$$

The kinetic energy metric is, therefore,

$$\mathbb{G} = m(dx \otimes dx + dy \otimes dy) + I_{body}(d\theta \otimes d\theta) + J_{roll}(d\psi_R \otimes d\psi_R + d\psi_L \otimes d\psi_L). \quad (5.4.7)$$

•

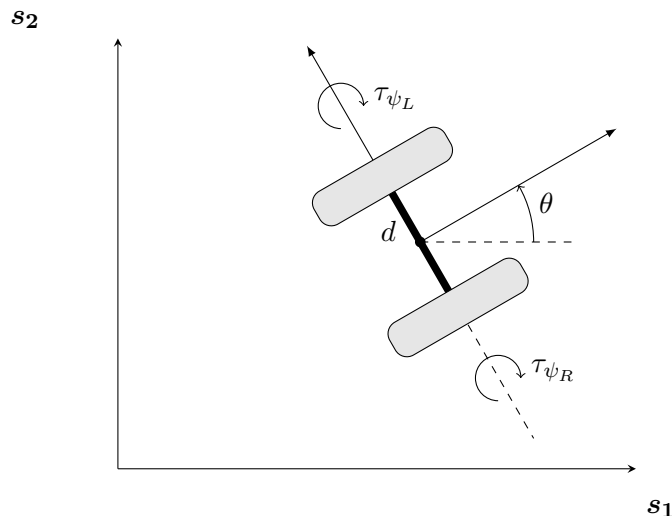


Figure 5.2: Two-wheeled robot forces.

Example 5.4.6 (Two-wheeled robot forces). As per Figure 5.2, the forces acting on the two-wheeled robot are torques represented by

$$F^1 = \tau_{\psi_R} (0, 0, 0, 1, 0) = \tau_{\psi_R} d\psi_R, \quad F^2 = \tau_{\psi_L} (0, 0, 0, 0, 1) = \tau_{\psi_L} d\psi_L,$$

with τ_{ψ_R} and τ_{ψ_L} defined on $\mathbb{R} \times \mathbb{TQ}$. •

Example 5.4.7 (Two-wheeled robot orthogonal projections). The orthogonal projections, $P_{\mathcal{D}}$ and $P_{\mathcal{D}}^\perp$, can be calculated using the distribution from Example 5.2.4 and the the Riemannian as per Equation (5.4.5). We do not write out this computation. •

Example 5.4.8 (Two-wheeled robot equations of motion). Recall our expressions for \mathbb{G} , $P_{\mathcal{D}}$, $P_{\mathcal{D}}^\perp$, F^1 , F^2 , and let $\lambda^1, \lambda^2, \lambda^3 \in \mathbb{R}$. The local representation of the equations of motion are

$$\begin{aligned} \ddot{x} &= \frac{1}{m} \lambda^1, \quad \ddot{y} = \frac{1}{m} \lambda^2, \quad \ddot{\theta} = \frac{1}{I_{body}} \lambda^3, \\ \ddot{\psi}_R &= \frac{1}{J_{roll}} \tau_{\psi_R} - \frac{\rho}{2J_{roll}} \cos \theta \lambda^1 - \frac{\rho}{2J_{roll}} \sin \theta \lambda^2 - \frac{\rho}{dJ_{roll}} \lambda^3, \\ \ddot{\psi}_L &= \frac{1}{J_{roll}} \tau_{\psi_L} - \frac{\rho}{2J_{roll}} \cos \theta \lambda^1 - \frac{\rho}{2J_{roll}} \sin \theta \lambda^2 + \frac{\rho}{dJ_{roll}} \lambda^3, \\ \dot{x} &= \frac{\rho}{2} (\dot{\psi}_R + \dot{\psi}_L) \cos \theta, \quad \dot{y} = \frac{\rho}{2} (\dot{\psi}_R + \dot{\psi}_L) \sin \theta, \quad \dot{\theta} = \frac{\rho}{d} (\dot{\psi}_R - \dot{\psi}_L). \end{aligned} \quad (5.4.8)$$

Solving for $\lambda^1, \lambda^2, \lambda^3 \in \mathbb{R}$, the local representation of Equation (4.4.4) for the two-

wheeled robot is

$$\begin{aligned}
\ddot{x} &= \frac{\rho \cos \theta}{m\rho^2 + 2J_{roll}} (\tau_{\psi_R} + \tau_{\psi_L}) - \rho\dot{\theta} \left(\frac{\dot{\psi}_R + \dot{\psi}_L}{2} \right) \sin \theta, \\
\ddot{y} &= \frac{\rho \sin \theta}{m\rho^2 + 2J_{roll}} (\tau_{\psi_R} + \tau_{\psi_L}) + \rho\dot{\theta} \left(\frac{\dot{\psi}_R + \dot{\psi}_L}{2} \right) \cos \theta, \\
\ddot{\theta} &= \frac{\rho d}{2I_{body}\rho^2 + J_{roll}d^2} (\tau_{\psi_R} - \tau_{\psi_L}), \\
\ddot{\psi}_R &= \frac{(4J_{roll}d^2 + \rho^2 (md^2 + 4I_{body})) \tau_{\psi_R} - \rho^2 (md^2 - 4I_{body}) \tau_{\psi_L}}{2(m\rho^2 + 2J_{roll})(2I_{body}\rho^2 + J_{roll}d^2)}, \\
\ddot{\psi}_L &= \frac{(4J_{roll}d^2 + \rho^2 (md^2 + 4I_{body})) \tau_{\psi_R} - \rho^2 (md^2 - 4I_{body}) \tau_{\psi_L}}{2(m\rho^2 + 2J_{roll})(2I_{body}\rho^2 + J_{roll}d^2)}. \tag{5.4.9}
\end{aligned}$$

•

Chapter 6

Control design using virtual surfaces

We are now ready to design control forces to make the physical system behave in a desirable way. The method we explore is to design a virtual surface (or potential function) that the vehicle will naturally “fall” down due to the induced virtual potential force.

In this method, we aim to characterise the virtual potential function solely by the spatial group coordinates as this represents where we want the body to go (or not go). For example, we can place a minima at a coordinate the body should travel to, while a maxima can be placed at point we want to avoid. This can be seen as a method of potential shaping, but we are translating a virtual potential force and its influence on the virtual system to physical control forces.

Also, we design a virtual force that steers the system in directions complementary to the force generated by the virtual potential force. We can then compute the control forces, F , so that the physical system follows the same trajectory.

Finally, using the rolling disk as an example, we prescribe surfaces to perform point stabilisation, path tracking, and obstacle avoidance.

6.1. The physical system

Suppose that we have a simple mechanical system $(\mathbb{Q}, \mathbb{G}, F, \mathcal{D})$ on a principal bundle $(\mathbb{Q}, \mathbb{M}, \mathbb{G}, \pi)$. Let \mathbb{M} have coordinates that represent the actuated degrees of freedom of the body.

Since the physical control inputs $F(t, x, g) \in T_x^* \mathbb{M}$, the trajectories of the group coordinates in \mathbb{G} are solely characterised by the trajectories of the base coordinates. We can fully determine the motion of the body via the constraints which comprise a connection on \mathbb{Q} .

Now, let us write down a few facts about \mathbb{Q} , and the decompositions of $T\mathbb{Q}$ and $T^*\mathbb{Q}$:

- (i) Since $\mathbb{Q} = \mathbb{M} \times \mathbb{G}$ is a principal fibre bundle, $T\mathbb{Q} = T\mathbb{M} \oplus T\mathbb{G}$ and $T\mathbb{Q} = \mathcal{D} \oplus \mathcal{D}^\perp$.
- (ii) Further, $T^*\mathbb{Q} = T^*\mathbb{M} \oplus T^*\mathbb{G} = T^*\mathbb{M} \oplus \text{ann}(T\mathbb{M}) = \text{ann}(T\mathbb{G}) \oplus T^*\mathbb{G}$, and $T^*\mathbb{Q} = \text{ann}(\mathcal{D}^\perp) \oplus \text{ann}(\mathcal{D})$.

The decompositions result from the fact we have two representations of subspaces that form the tangent space. The two distributions, \mathcal{D} , and \mathcal{D}^\perp , span the tangent space. The

tangent space is also spanned by the tangent space of the base and group manifolds. We assume that we can determine the required components of the virtual force because representations of the tangent space are, in general, not equal due to the non-integrability of the distribution.

Recall the global equations of motion (given in Equation (4.4.4)) are

$$\nabla_{\gamma'(t)}^{\mathbb{G}} \gamma'(t) = P_{\mathcal{D}} \left(\mathbb{G}^{\sharp} (F(t, \gamma'(t))) \right) - \left(\nabla_{\gamma'(t)}^{\mathbb{G}} P_{\mathcal{D}}^{\perp} \right) (\gamma'(t)).$$

Since, by construction of \mathbb{M} , the physical input forces are independent and span the base cotangent space, then it is true that

$$\left\{ P_{\mathcal{D}} \left(\mathbb{G}^{\sharp} (F(t, \gamma'(t))) \right) : F(t, \gamma'(t)) \in \mathbb{T}^*\mathbb{M} \right\} = \mathcal{D}.$$

To design the physical input forces, F , and ultimately make our system behave in a useful way, we turn our attention to a virtual system.

6.2. The virtual system

Definition 6.2.1 (The virtual system). Let $(\mathbb{Q}, \mathbb{G}, V^*, \tilde{F}, \mathcal{D})$ be a virtual simple mechanical system on a principal bundle $(\mathbb{Q}, \mathbb{M}, \mathbb{G}, \pi)$ where

- (i) \mathbb{Q} is the configuration manifold (of the physical simple mechanical system),
- (ii) \mathbb{G} is the Riemannian metric (of the physical simple mechanical system),
- (iii) $V^* \in C^\infty(\mathbb{G})$ is a user-defined virtual potential function on \mathbb{G} ,
- (iv) \tilde{F} is a C^∞ -force comprised of a virtual force, F^* , and a dissipative force, F_d ,¹ and
- (v) \mathcal{D} is the distribution (of the physical simple mechanical system).

Firstly, we determine the virtual equations of motion. We refer the reader to [6] for further detail on potential functions, potential forces, and dissipative forces.

A *virtual potential function* $V^* \in C^\infty(\mathbb{G})$ on \mathbb{G} generates a *virtual potential force* given by

$$F_{V^*}^*(t, v_g) = -dV^*(g) = -\frac{\partial V^*(g)}{\partial g^i} dg^i = -dV_{g^i}^*(g) dg^i \in \mathbb{T}_g^*\mathbb{G}. \quad (6.2.1)$$

The *virtual force* is a *designed* input and has the form

$$F^*(t, v_q) \in \mathbb{T}_q^*\mathbb{Q}. \quad (6.2.2)$$

We will outline some sufficient conditions to determine the necessary components of F^* , and a methodology to design the components.

Finally, we introduce a *dissipative force*, which acts solely to remove energy from the system in the actuated coordinates.

¹The dissipative force is not necessary to actuate the system, and is simply used to remove energy from the system, and thus converge to a minima.

Definition 6.2.2 (Dissipative force). A time-independent force $F: \mathbb{T}\mathbb{Q} \rightarrow \mathbb{T}^*\mathbb{Q}$ is *dissipative* if $\langle F(v_q); v_q \rangle \leq 0$ for each $v_q \in \mathbb{T}\mathbb{Q}$, and is *strictly dissipative* if it is dissipative and if $\langle F(v_q); v_q \rangle = 0$ only when $v_q \in Z(\mathbb{T}\mathbb{Q})$. •

Definition 6.2.3 (Rayleigh dissipation). Let \mathbb{Q} be a C^∞ -manifold. A *Rayleigh dissipation function* is a class C^∞ , symmetric, positive-semidefinite $(0,2)$ -tensor field R_{diss} on \mathbb{Q} . If R_{diss} is positive-definite, then it is *strict*. The dissipative force associated with a Rayleigh dissipation function is the map $-R_{diss}^b: \mathbb{T}\mathbb{Q} \rightarrow \mathbb{T}^*\mathbb{Q}$. A time-independent force $F: \mathbb{T}\mathbb{Q} \rightarrow \mathbb{T}^*\mathbb{Q}$ is *dissipative* if $\langle F(v_q); v_q \rangle \leq 0$ for each $v_q \in \mathbb{Q}$, and is *strictly dissipative* if it is dissipative and if $\langle F(v_q); v_q \rangle = 0$ only when $v_q \in Z(\mathbb{T}\mathbb{Q})$. •

Let $F_d: \mathbb{T}\mathbb{Q} \rightarrow \mathbb{T}^*\mathbb{Q}$ be a time-independent C^∞ -dissipative force given by

$$F_d(\gamma'(t)) = -R_{diss}^b(\gamma'(t), \gamma'(t)).$$

6.2.1. The virtual equations of motion

Using expressions of the virtual surface, dissipative force, and virtual force, the global equations of motion become

$$\mathbb{G}_{\nabla_{\tilde{\gamma}'(t)}\tilde{\gamma}'(t)} = \mathbb{G}^\sharp \left(-dV^*(\tilde{\gamma}(t)) + \underbrace{F_d(\tilde{\gamma}'(t)) + F^*(t, \tilde{\gamma}'(t))}_{\tilde{F}(t, \tilde{\gamma}(t), \tilde{\gamma}'(t))} \right) + \lambda^*(t), \quad (6.2.3)$$

$$P_{\mathcal{D}}^\perp(\tilde{\gamma}'(t)) = 0, \quad (6.2.4)$$

where $\lambda^*(t) \in \mathcal{D}^\perp$ is the virtual constraint force, and $\tilde{\gamma}: [a, b] \rightarrow \mathbb{Q}$ is the virtual trajectory of the system.

The constrained equations of motion of the virtual system are

$$\mathbb{G}_{\nabla_{\tilde{\gamma}'(t)}\tilde{\gamma}'(t)} = P_{\mathcal{D}} \left(\mathbb{G}^\sharp \left(-dV^*(\tilde{\gamma}(t)) + \tilde{F}(t, \tilde{\gamma}(t), \tilde{\gamma}'(t)) \right) \right) - \left(\mathbb{G}_{\nabla_{\tilde{\gamma}'(t)}P_{\mathcal{D}}^\perp} \right) (\tilde{\gamma}'(t)). \quad (6.2.5)$$

6.2.2. Determining the components of the virtual force

Using the equations of motion, we can give some properties of the virtual potential force and the components of the virtual force.

Due to the product structure of \mathbb{Q} , it holds that $dV^*(\tilde{\gamma}(t)) \in \mathbb{T}^*\mathbb{G} = \text{ann}(\mathbb{T}\mathbb{M})$. The orthogonal projection of the set $\mathbb{T}^*\mathbb{G}$ maps to a subset of the distribution, i.e., $P_{\mathcal{D}}(\mathbb{G}^\sharp(\mathbb{T}^*\mathbb{G})) \subseteq \mathcal{D}$.

We assume that there always exists a subgroup $\mathbb{H} \subseteq \mathbb{G}$ such that $P_{\mathcal{D}}(\mathbb{G}^\sharp(\mathbb{T}^*\mathbb{H})) \subset \mathcal{D}$. We acknowledge that this strict inclusion is also dependent on the components of the Riemannian metric, \mathbb{G} .

Therefore, it follows that

$$\dim \left(P_{\mathcal{D}} \left(\mathbb{G}^\sharp(\mathbb{T}^*\mathbb{H}) \right) \right) < \dim(\mathcal{D}).$$

Thus, there exists a *complementary force set*, $C_{\mathcal{F}}$, with $\dim(C_{\mathcal{F}}) > 0$, such that

$$C_{\mathcal{F}} \oplus P_{\mathcal{D}} \left(\mathbb{G}^\sharp(\mathbb{T}^*\mathbb{H}) \right) = \mathcal{D} \implies \dim(C_{\mathcal{F}}) + \dim \left(P_{\mathcal{D}} \left(\mathbb{G}^\sharp(\mathbb{T}^*\mathbb{H}) \right) \right) = \dim(\mathcal{D}).$$

This is equivalent to ensuring

$$\text{span} \left\{ C_{\mathcal{F}}, P_{\mathcal{D}} \left(\mathbb{G}^{\sharp} (\mathbb{T}^* \mathbb{H}) \right) \right\} = \mathcal{D}. \quad (6.2.6)$$

Similar to the physical system, we require

$$\left\{ P_{\mathcal{D}} \left(\mathbb{G}^{\sharp} \left(-dV^* (\tilde{\gamma}(t)) + \tilde{F}(t, \tilde{\gamma}(t), \tilde{\gamma}'(t)) \right) \right) : dV^* (\tilde{\gamma}(t)) \in \mathbb{T}^* \mathbb{H}, \tilde{F}(t, \tilde{\gamma}(t), \tilde{\gamma}'(t)) \in \mathbb{T}^* \mathbb{Q} \right\} = \mathcal{D},$$

or

$$\text{span} \left\{ P_{\mathcal{D}} \left(-\mathbb{G}^{\sharp} dV^* (\tilde{\gamma}(t)) \right), P_{\mathcal{D}} \left(\mathbb{G}^{\sharp} \left(\tilde{F}(t, \tilde{\gamma}(t), \tilde{\gamma}'(t)) \right) \right) \right\} = \mathcal{D}.$$

Therefore, the components of \tilde{F} can be chosen such that

$$\left\{ P_{\mathcal{D}} \left(\mathbb{G}^{\sharp} \left(\tilde{F}(t, \tilde{\gamma}(t), \tilde{\gamma}'(t)) \right) \right) \right\} \in C_{\mathcal{F}}.$$

It follows that the components of \tilde{F} are only required in directions complementary to the direction of the force generated by the virtual potential function. Since F_d is strictly dissipative, we ensure Equation (6.2.6) holds by specifying the components of F^* in directions complementary to the direction of the force generated by the virtual potential function.

From a virtual system to physical control inputs

Given a virtual simple mechanical system $(\mathbb{Q}, \mathbb{G}, V^*, \tilde{F}, \mathcal{D})$ with trajectory $\tilde{\gamma}: [a, b] \rightarrow \mathbb{Q}$. Let $V^* \in C^\infty(\mathbb{H})$, where $\mathbb{H} \subseteq \mathbb{G}$, and $\tilde{F} \in \mathbb{T}^* \mathbb{Q}$ be chosen as above. Then the physical simple mechanical system $(\mathbb{Q}, \mathbb{G}, F, \mathcal{D})$ will follow the trajectory $\gamma(t) = \tilde{\gamma}(t)$ if

$$P_{\mathcal{D}} \left(\mathbb{G}^{\sharp} (F(t, \gamma'(t))) \right) = P_{\mathcal{D}} \left(\mathbb{G}^{\sharp} \left(-dV^* (\gamma(t)) + \tilde{F}(t, \gamma(t), \gamma'(t)) \right) \right). \quad (6.2.7)$$

6.3. Controlling the rolling disk

Recall, the physical system is defined by $(\mathbb{Q}, \mathbb{G}, F, \mathcal{D})$, on a principal bundle $(\mathbb{Q}, \mathbb{M} = \mathbb{S}^1 \times \mathbb{S}^1, \mathbb{G} = \mathbb{R}^2, \pi)$ where

- (i) $\mathbb{Q} = \mathbb{S}^1 \times \mathbb{S}^1 \times \mathbb{R}^2$,
- (ii) $\mathbb{G} = m(dx \otimes dx + dy \otimes dy) + J_{spin}(d\theta \otimes d\theta) + J_{roll}(d\phi \otimes d\phi)$,
- (iii) $F = \tau_\theta d\theta + \tau_\phi d\phi \in \mathbb{T}^* \mathbb{M}$ (the physical control forces), and
- (iv) $\mathcal{D} = \text{span} \left\{ X_1 = \rho \cos \theta \frac{\partial}{\partial x} + \rho \sin \theta \frac{\partial}{\partial y} + \frac{\partial}{\partial \phi}, X_2 = \frac{\partial}{\partial \theta} \right\} \subset \mathbb{T}\mathbb{Q}$.

The global equations of motion of the physical system are given by Equation (4.4.4), where $\gamma: [a, b] \rightarrow \mathbb{Q}$ is the trajectory of the system.

Figure 6.1 shows a disk, with base configuration $x = (\phi, \theta) \in \mathbb{M}$ and group configuration $g = (x, y) \in \mathbb{G}$, rolling on a virtual surface V^* , with local slope dV^* . With this information, the virtual disk is defined by $(\mathbb{Q}, \mathbb{G}, V^*, \tilde{F}, \mathcal{D})$, where

- (i) $\mathbb{Q} = \mathbb{S}^1 \times \mathbb{S}^1 \times \mathbb{R}^2$,

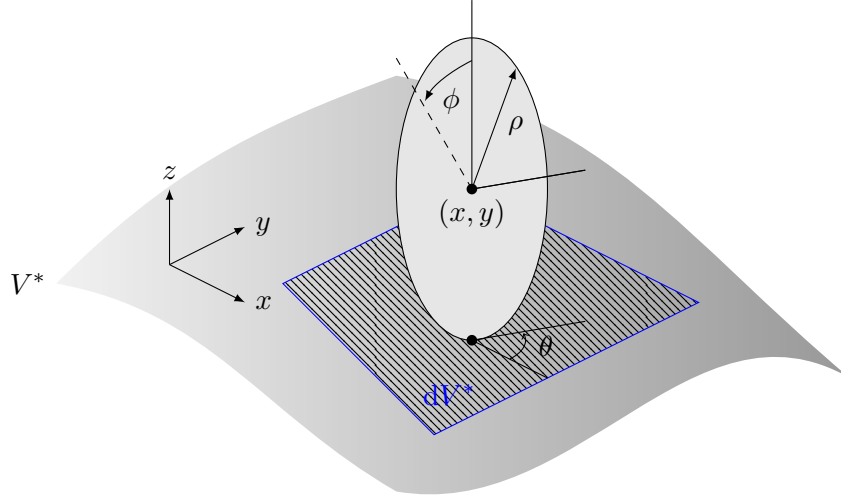


Figure 6.1: A rolling disk on a virtual surface

- (ii) $\mathbb{G} = m(dx \otimes dx + dy \otimes dy) + J_{spin}(d\theta \otimes d\theta) + J_{roll}(d\phi \otimes d\phi)$,
- (iii) $V^* \in C^\infty(\mathbb{G})$ is a user-defined virtual potential function on \mathbb{G} ,²
- (iv) $\tilde{F} = F_d + F^* = (F_{d_\theta} + F_\theta^*)d\theta + (F_{d_\phi} + F_\phi^*)d\phi \in \mathbb{T}^*\mathbb{M}$ (a dissipative force and virtual force), and
- (v) $\mathcal{D} = \text{span} \left\{ X_1 = \rho \cos \theta \frac{\partial}{\partial x} + \rho \sin \theta \frac{\partial}{\partial y} + \frac{\partial}{\partial \phi}, X_2 = \frac{\partial}{\partial \theta} \right\} \subset \mathbb{T}\mathbb{Q}$.

The global equations of motion of the physical system are given by Equation (6.2.5), where $\tilde{\gamma}: [a, b] \rightarrow \mathbb{Q}$ is the virtual trajectory of the system.

We concern ourselves with the choice of a virtual surface V^* , the choice of the components of the virtual force, F^* , and subsequently the design of the components to induce “useful” trajectory on the system.

6.3.1. Determining the components of the virtual force for the rolling disk

Considering $dV^* = dV_x^*dx + dV_y^*dy \in \mathbb{T}^*\mathbb{G}$, a computation shows that $P_{\mathcal{D}}(\mathbb{G}^\#(dV^*))$ has components only in the span of $X_1 \in \mathcal{D}$. Thus, we need to design a virtual force to spin the disk in the direction of $X_2 \in \mathcal{D}$. Thus, for the rolling disk we take $C_{\mathcal{F}} \in \text{span}\{X_2\}$, which implies $F^* = F_\theta^*d\theta = \tau^*d\theta \in \mathbb{T}^*\mathbb{M}$, i.e., a torque that spins the disk about its vertical axis.

6.3.2. Forced equations of motion

We now obtain the general equations of motion of the system in coordinates, and solve for the physical control inputs, $F = \tau_\theta d\theta + \tau_\phi d\phi \in \mathbb{T}^*\mathbb{M} \subseteq \mathbb{T}^*\mathbb{Q}$. Let

²For the rolling disk, the subgroup $\mathbb{H} = \mathbb{R}^2 = \mathbb{G}$. For the two-wheeled robot the subgroup $\mathbb{H} = \mathbb{R}^2 \subset \mathbb{G}$. In both cases, \mathbb{H} represents the spatial coordinates of the body. There is some interesting geometry occurring here that should be studied further.

- (i) $V^* \in C^\infty(\mathbf{G})$;
- (ii) $dV^* = dV_x^* dx + dV_y^* dy \in \mathbb{T}^*\mathbf{G}$;
- (iii) $F_d = -(F_{d_\phi} d\phi + F_{d_\theta} d\theta) \in \mathbb{T}^*\mathbf{M}$;
- (iv) $F^* = \tau^* d\theta \in \mathbb{T}^*\mathbf{M}$.

Then, by Equation (6.2.7),

$$P_{\mathcal{D}} \left(\frac{1}{J_{spin}} \tau_\theta \frac{\partial}{\partial \theta} + \frac{1}{J_{roll}} \tau_\phi \frac{\partial}{\partial \phi} \right) = P_{\mathcal{D}} \left(-\frac{1}{m} \left(dV_x^* \frac{\partial}{\partial x} + dV_y^* \frac{\partial}{\partial y} \right) - \frac{1}{J_{spin}} (F_{d_\theta} - \tau^*) \frac{\partial}{\partial \theta} - \frac{1}{J_{roll}} F_{d_\phi} \frac{\partial}{\partial \phi} \right).$$

Thus, the physical control inputs are

$$\tau_\theta = -F_{d_\theta} + \tau^*, \quad (6.3.1)$$

$$\tau_\phi = -F_{d_\phi} - \rho(dV_x^* \cos \theta + dV_y^* \sin \theta), \quad (6.3.2)$$

and the overall equations of motion of the physical system are

$$\begin{aligned} \ddot{x} &= -\frac{\rho \cos \theta}{m\rho^2 + J_{roll}} (F_{d_\phi} + \rho(dV_x^* \cos \theta + dV_y^* \sin \theta)) - \rho \dot{\theta} \dot{\phi} \sin \theta, \\ \ddot{y} &= -\frac{\rho \sin \theta}{m\rho^2 + J_{roll}} (F_{d_\phi} + \rho(dV_x^* \cos \theta + dV_y^* \sin \theta)) + \rho \dot{\theta} \dot{\phi} \cos \theta, \\ \ddot{\theta} &= -\frac{1}{J_{spin}} (F_{d_\theta} - \tau^*), \\ \ddot{\phi} &= -\frac{1}{m\rho^2 + J_{roll}} (F_{d_\phi} + \rho(dV_x^* \cos \theta + dV_y^* \sin \theta)). \end{aligned} \quad (6.3.3)$$

6.4. Designing the virtual force

As the goal is the design a virtual force that spins the disk, we impose the following assumptions on the virtual disk:

1. the disk is perpendicular to the virtual surface;
2. the disk has a virtual mass, $m^* \in \mathbb{R}_{\geq 0}$, that is acted on by a virtual gravity, $g^* \in \mathbb{R}_{\geq 0}$. The virtual gravitational force $m^* g^*$ acts vertically;
3. the disk has a virtual centre of mass, G^* , located at $\mathbf{l}^* = (l^* \cos \theta, l^* \sin \theta, \rho) \in \mathbb{R}^3$ from the physical centre of mass $G = (x, y, \rho) \in \mathbb{R}^3$, with magnitude $l^* \in \mathbb{R}$;
4. the virtual gravitational force generated through the virtual centre of mass induces a virtual torque about the physical centre of mass;
5. the virtual force, f^* , is the component of the the virtual gravitational force parallel to the virtual slope.

Figure 6.2 illustrates assumptions 1 and 2, and Figure 6.3 shows assumptions 3 and 5. Employing these assumptions, we can design the component of the virtual force for each spatial group variable.

We design the components of the virtual force by making the following observations:

1. The tangent of the angle, $\psi_x \in \mathbb{R}$, the disk forms with the vertical is equal to the local virtual slope in the x -coordinate. The local slope equal to the component of the virtual potential force for that coordinate, i.e.,

$$\tan \psi_x = -\frac{\partial V^*}{\partial x} = -dV_x^*.$$

2. Thus, the angle the virtual surface forms with the global x -axis is

$$\psi_x = -\tan^{-1}(dV_x^*).$$

3. Since the virtual gravitational force is vertical by Assumption 2, we apply Assumption 5 to obtain the dx component of the virtual force as

$$f_x^* = m^* g^* \sin \psi_x = m^* g^* \sin(-\tan^{-1}(dV_x^*)) = -m^* g^* \frac{dV_x^*}{\sqrt{(dV_x^*)^2 + 1}} \in \mathbb{R}.$$

The derivation is the similar for the dy component.

4. The overall virtual force is $f^* = f_x^* dx + f_y^* dy \in \mathbb{T}^*G$.
5. The total external virtual force, F^* , that acts on the disk is

$$F^* = \left\langle f^*; \frac{d\mathbf{l}^*}{dt} \right\rangle = -l^* (-f_x^* \sin \theta + f_y^* \cos \theta) d\theta = \tau^* d\theta \in \mathbb{T}^*M. \quad (6.4.1)$$

6. Substituting the components from Equation (3) into Equation (6.4.1) gives

$$\begin{aligned} \tau^* &= -m^* g^* l^* \left(-\sin \theta \frac{dV_x^*}{\sqrt{(dV_x^*)^2 + 1}} + \cos \theta \frac{dV_y^*}{\sqrt{(dV_y^*)^2 + 1}} \right) \\ &= -K^* \left(-\sin \theta \frac{dV_x^*}{\sqrt{(dV_x^*)^2 + 1}} + \cos \theta \frac{dV_y^*}{\sqrt{(dV_y^*)^2 + 1}} \right), \end{aligned} \quad (6.4.2)$$

where $K^* \in \mathbb{R}$ is a tuneable control parameter that represents the virtual mass, gravity and distance from the physical centre of mass.

Example 6.4.1 (The rolling disk). Let $V^*(g) = \frac{1}{2}(x^2 + y^2)$, then $dV^*(g) = xdx + ydy$. Let $R_{diss}^b = (d\phi \otimes d\phi + d\theta \otimes d\theta)$. Let the virtual constant $K^* = 1$.

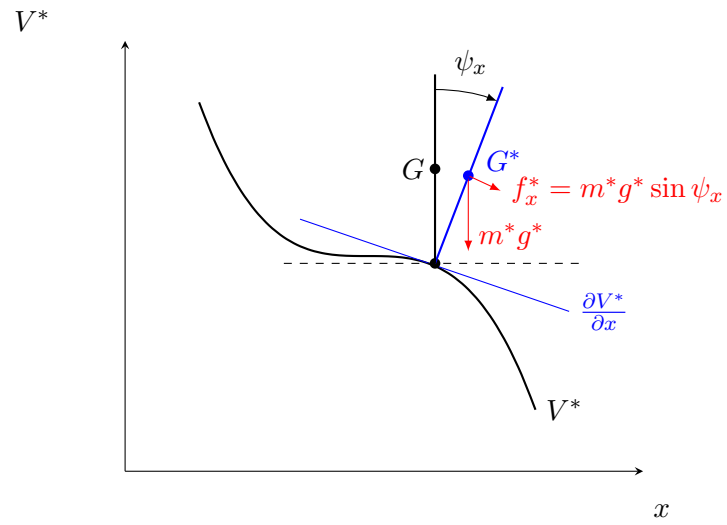


Figure 6.2: The disk normal to the virtual surface

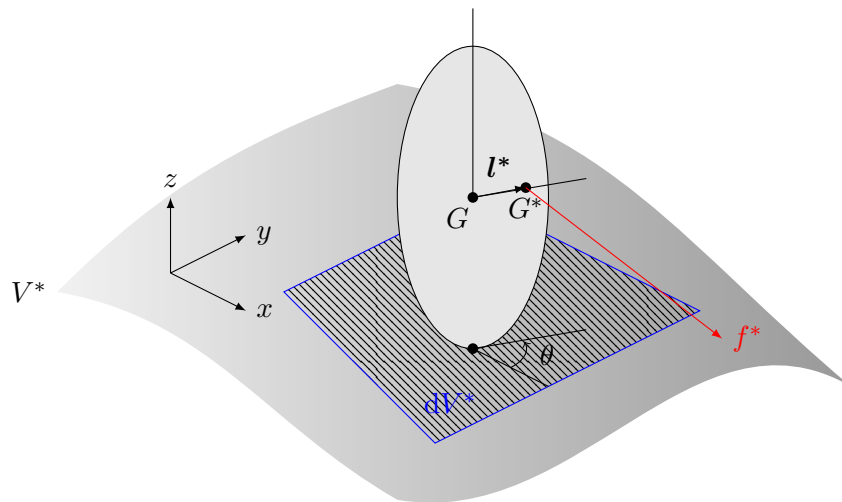


Figure 6.3: A rolling disk with a virtual force



Figure 6.4: Simulation of Equation (6.4.3) with $V^*(g) = \frac{1}{2}(x^2 + y^2)$, $a = 1$, and $K^* = 1$

Substituting this information into Equation (6.3.3) gives the equations of motion of the physical system as

$$\begin{aligned}
 \ddot{x} &= -\frac{\rho \cos \theta}{m\rho^2 + J_{roll}} \left(\dot{\phi} + \rho(x \cos \theta + y \sin \theta) \right) - \rho \dot{\theta} \dot{\phi} \sin \theta, \\
 \ddot{y} &= -\frac{\rho \sin \theta}{m\rho^2 + J_{roll}} \left(\dot{\phi} + \rho(x \cos \theta + y \sin \theta) \right) + \rho \dot{\theta} \dot{\phi} \cos \theta, \\
 \ddot{\theta} &= -\frac{1}{J_{spin}} \left(\dot{\theta} + \left(-\sin \theta \frac{x}{\sqrt{x^2 + 1}} + \cos \theta \frac{y}{\sqrt{y^2 + 1}} \right) \right), \\
 \ddot{\phi} &= -\frac{1}{m\rho^2 + J_{roll}} \left(\dot{\phi} + \rho(x \cos \theta + y \sin \theta) \right). \tag{6.4.3}
 \end{aligned}$$

Figure 6.4, demonstrates the trajectories of Equation (6.4.3) from rest, initial configuration $q(0) = (-6, 4, \frac{\pi}{3}, 0)$. Note that, this choice of V^* implies we want $(x_f, y_f) = (0, 0)$.

It is evident that the group coordinates (x, y) asymptotically go to zero. The base coordinate, θ , converges to an arbitrary value. In a physical application, we can make two actions to compensate for this: orient the disk when the final group coordinate is reached, or simply turn the controls “off”.

While we have not given any thought to how a and K^* are chosen, this scheme clearly steers the disk from our initial position, to the group origin.

Depending on the application, these parameters can be determined by assessing the stability of the system (and find bounds on the tuneable control parameters), but there are instances where the notion of stability is not immediately clear, i.e., when tracking a path we never want the system to be at rest, or at an equilibrium configuration, so how does one assess “stability”, or convergence?

As per [16], for dissipative nonholonomic mechanical systems, we know that equilibria can arise at configurations which are not critical points of the potential function (in this case the virtual potential function). This already presents a huge limitation; in order to easily apply Lyapunov methods, we need to restrict ourselves to equilibria which are critical points.

6.5. Designing practical surfaces

We are now ready to design a collection of surfaces that ensures our system behaves in a useful way. Since we have established that the rolling disk is controllable, and that we can

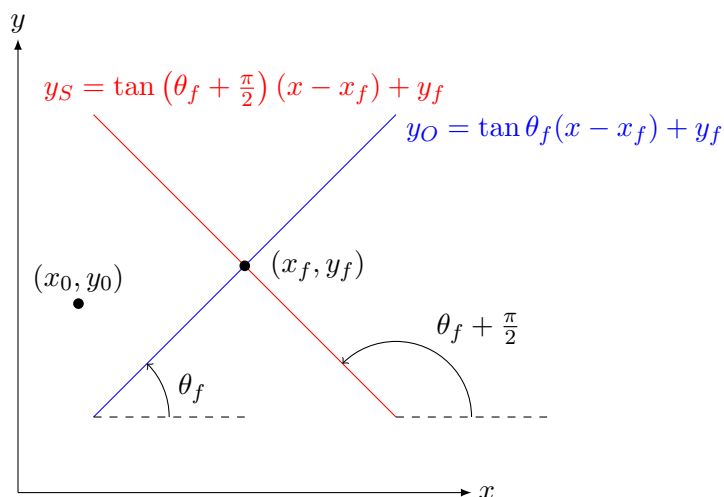


Figure 6.5: The lines forming the minina of virtual surfaces

design virtual surfaces that actuate the system in the base variables that are solely characterised by the group coordinates (x, y) , we can design surfaces to influence the behaviour of our system. Furthermore, we want to ensure convergence to a specified orientation, θ , of the disk.

Thus, we are tasked with finding a set of surfaces that solve two fundamental control problems—point stabilisation and path tracking. We also investigate obstacle avoidance as the end goal is to be able to compute control inputs for a vehicle in a dynamic environment.

6.5.1. Point stabilisation

In our setting, point stabilisation is akin to the virtual disk rolling to a minimum on the virtual surface. Point stabilization for nonholonomic vehicles is well studied, and we highlight the main result that it is not possible to prescribe a continuous control so that a vehicle at rest with configuration q_0 at time $T = 0$, is also at rest at its final configuration q_f at some time $T > 0$. Acknowledging this allows us to tackle the problem in a logical way, i.e., specifying piecewise continuous control inputs with switching. This ultimately leads to the *Orient-Settle* control strategy.

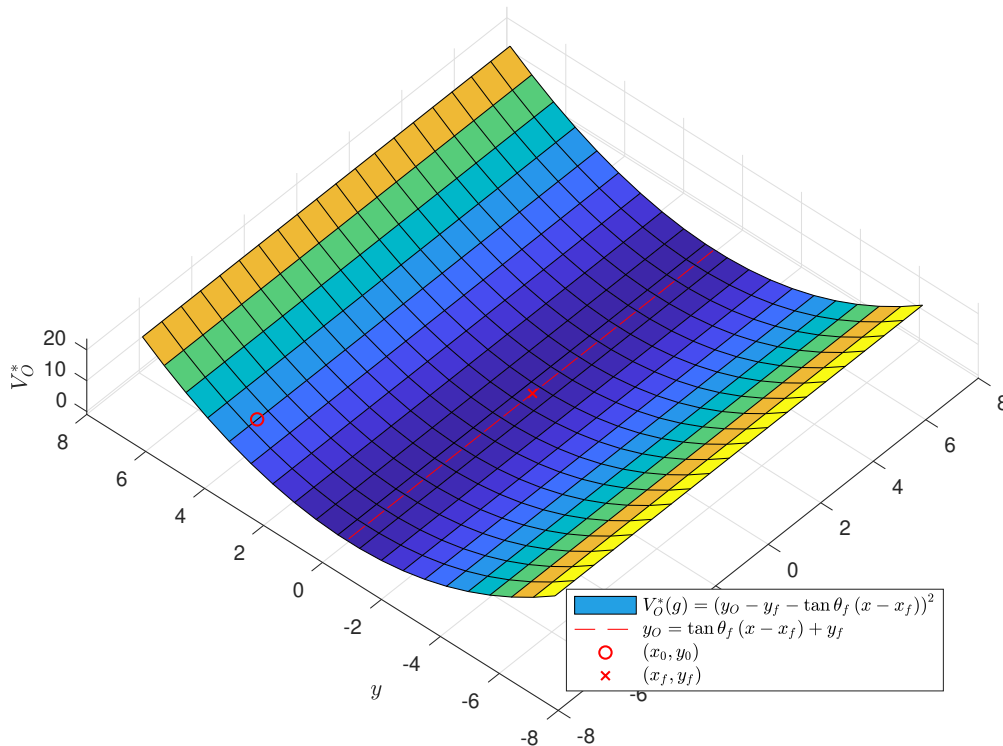
This scheme uses the idea that the final configuration $(x_f, y_f, \theta_f, \phi_f)$ is fully captured by a line in $\mathbf{G} = \mathbb{R}^2$ given by $x \mapsto \tan \theta_f(x - x_f) + y_f$, which is solely a function of the group configuration at any given time.³

Figure 6.5 demonstrates the two lines that form the minimums of parabolas used in this control strategy. Since the line in the plane can be parameterised by $(x, y = f(x)) \in \mathbb{R}^2$, the virtual surface about this line is $V^*(g) = \frac{1}{2}(y - f(x))^2$.

This scheme has two phases:

Orient With $K^* > 0$, the vehicle *orients* itself in a parabola (with minina along the line with

³We acknowledge that $\tan(x)$ is undefined when $x = \frac{\pi}{2} + \pi k, k \in \mathbb{Z}$. In simulations, one can account for this rather easily.


 Figure 6.6: The *orient* phase virtual surface

angle θ_f) represented by the surface

$$V_O^*(g) = \frac{1}{2} (y_O - y_f - \tan \theta_f (x - x_f))^2.$$

An example of this surface is plotted in Figure 6.6 for $(x_0, y_0) = (-6, 4)$ and $(x_f, y_f) = (0, 0)$ and $\theta_f = 0$.

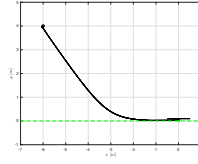
Settle Once the disk angle has converged to θ_f , the disk then *settles* in a parabola along a line given by $x \mapsto \tan(\theta_f + \frac{\pi}{2})(x - x_f) + y_f$. This surface is given by

$$V_S^*(g) = \frac{1}{2} \left(y_S - y_f - \tan(\theta_f + \frac{\pi}{2})(x - x_f) \right)^2$$

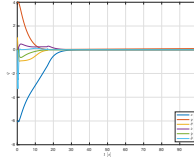
and $K^* = 0$.

The results are demonstrated in Figure 6.7.

The switching strategy between the control inputs is dependent on the error of the controlled coordinate for that surface. In theory, we switch controls when $\lim_{t \rightarrow \infty} q^i(t) - q_f^i(t) = 0$, for $q^i \in (x, y, \theta)$, however this is not practical numerically, so we define error bounds, $\epsilon_{q^i} \in \mathbb{R}_{>0}$, for the q^i -th coordinate to trigger the switch. These parameters require



(a) Trajectory plot.



(b) State plot.

Figure 6.7: *Orient-Settle* point stabilization technique. For the two phases, $a = \{2, 2\}$, and $K^* = \{6, 0\}$

tuning, but for the sake of this report we do not explore the choice or bounds of these switching constants. What we note, however, is that we never turn the controls off. They are only zero at the minimum of V^* .

Figure 6.7 demonstrates the *Orient-Settle* control strategy with $q_0 = (-6, 4, \frac{\pi}{3}, 0)$ and $q_f = (0, 0, 0, \star)$.⁴

All trajectories converge to the origin (within their associated error band) for a period of time. What is observable, however, is the motion away from the origin as time increases. This indicates the disk is not exactly at the origin (which would make the control inputs identically zero). Hence, we know we can make the configuration to asymptotically converge to the origin. In practice, the controls can be turned off when the system is within a prescribed error bound.

Since this is a dynamic simulation, the system still needs time to converge to the origin once the controls are zero (or turned off). The dissipative force ensures the convergence of the system to a minima (in this case the origin). In a kinematic simulation, a control input of zero would instantaneously stop the disk—a property that is impossible in a physical system.

6.5.2. Path tracking

In our setting, path tracking is equivalent to the virtual disk rolling along a path in the plane that is the minimum of a parabola at that point. Without loss of generality, assume we can define a path in the plane as $(x, y = f(x)) \in \mathbb{R}^2$, the virtual surface to track that path $V^*(g) = \frac{1}{2}(y - f(x))^2 - x$. Note, we add the $-x$ term to impart a velocity on the disk in the positive x -direction.⁵ We test the following paths:

PT-1 *A line*: Let $y = f(x) = 0$, then $V^*(g) = \frac{1}{2}y^2 - x$. Let $a = 2$, and $K^* = 6$. Figure 6.8 shows the result of this simulation. It is clear the disk tracks the reference path (within a certain margin of error).

PT-2 *Sine wave*: Let $y = f(x) = \sin(x)$, then

$$V^*(g) = \frac{1}{2}(y - \sin x)^2 - x.$$

Let $a = 2$, and $K^* = 6$. Figure 6.9 demonstrates the implementation of this path controller. The disk tracks the overall shape of reference path, but with a lag, due

⁴Since we are not concerned with the total angle the disk has rolled, ϕ_f is arbitrary.

⁵This term can be plane with slope in the direction of the path.



Figure 6.8: Tracking a straight path (PT-1)



Figure 6.9: Tracking a sine wave path (PT-2)

to the induction of velocity from the $-x$ term. Decreasing the magnitude of the $-x$ term decreases the lag error, but the vehicle does not traverse the overall shape as well.

6.5.3. Obstacle avoidance

Given an object at $(x_o, y_o) \in \mathbb{R}^2$, and disk position $(x, y) \in \mathbb{R}^2$, we can place a multivariate Gaussian function at the location of obstacle of the form

$$V^*(g) = \frac{\alpha}{2} \exp\left(-\frac{1}{\beta} ((x - x_o)^2 + (y - y_o)^2)\right),$$

where $\alpha, \beta \in \mathbb{R}$ are parameters that adjust the overall shape (height and width) of the function. A Gaussian function has some nice properties that make it a practical function to use for obstacle avoidance, including:

- the function is continuous;
- the value of the function decays exponentially to zero away from its origin, meaning far away from the obstacle, there is no contribution to the virtual surface;
- the derivative is easy to compute;
- we can manipulate certain parameters to change the shape and height of the function, i.e., the contribution to the surface;
- functions can be added linearly, allowing the surface for multiple objects to be determined efficiently.

Let us place three obstacles at $(10, 1)$, $(20, -1)$, $(30, 1)$, and let $\alpha = \beta = 1$. The resultant virtual surface is

$$V^*(g) = \frac{1}{2} \left(e^{-((x-1)^2+(y-10)^2)} + e^{-((x+1)^2+(y-20)^2)} + e^{-((x-1)^2+(y-30)^2)} \right) - x. \quad (6.5.1)$$

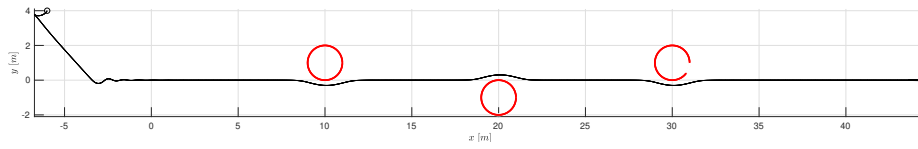


Figure 6.10: Obstacle avoidance trajectory

Figure 6.10 demonstrates the result of traversing the surface given by Equation (6.5.1), again with $q_0 = (-6, 4, \frac{\pi}{3}, 0)$. Again, we add the $-x$ term to impart a velocity on the disk. We can just as easily make this a function of the path we want the disk track.

Chapter 7

Conclusions and future work

7.1. Conclusions

In this report, we studied the connection between group and base variables in the presence of nonholonomic constraints. With knowledge of the controllability of a simple rolling disk, we then presented a framework to design virtual surfaces to achieve some simple, yet fundamental control tasks. Although there are still many unanswered questions, from this investigation we can summarize the following:

1. Representing the configuration of a rigid body as a group is a powerful way to determine the constraints, the constrained connection, and ultimately to determine the controllability of a system. We determine controllability using the Lie algebra rank condition.
2. The trivial principal bundle is not unique, and the associated connection one-form is also not unique. It is dependent on the choice of group and base variables and the corresponding group action. For simple mechanical systems, the most practical (and natural) principal fibre bundle is the one that separates the base and group variables by the actuated coordinates. This ensures the group variables are determined uniquely from the actual control inputs.
3. For any input force on a simple mechanical system, and the resulting external force on the constrained simple mechanical system is simply the orthogonal projection of the force. This allows us to use any “force” (whether designed or arbitrary) be a control input, and the system will satisfy its nonholonomic constraints and move accordingly. To determine the necessary components of the virtual force, we ensure the virtual force has dimension equal to the distribution along its trajectory, i.e., in directions complementary to the virtual potential force.
4. To stabilise the body to a point, the virtual potential function should be a function of the spatial group coordinates. To orient the body, the virtual potential function should be a function of the angle of the body.
5. It is possible to achieve point stabilization and path tracking for a rolling disk. The former cannot be done using a continuous control, but using piecewise continuous control inputs gives practical results.

6. The methodology works for avoiding obstacles.

7.2. Future work

In finishing this thesis, we have discovered some interesting geometry between the total configuration manifold, base space and group manifold and their connection to the distributions. It appears there is much to do to explore the intricacies of the relationships between their tangent and cotangent spaces in the presence of principal bundles and non-integrable distributions. The piece of this puzzle lies with the subgroup $\mathbf{H} \subseteq \mathbf{G}$, and therefore the intersection of \mathbf{TH} with the distribution, \mathcal{D} .

The one major omission from this report is a stability analysis. We picked a virtual surface in a logical way to make our system go to “low” areas and avoid “high” areas, but we never determined the requirements on the surface V^* based on a set of stability criteria. While this is relatively simple to do for our specific running example, a more thorough, generalized notion of these properties is a dissertation in itself.

Also, stability definitions for nonholonomic systems focus on the system being at an equilibrium point, a property that is undesirable when dealing with robot motion. An investigation into relative equilibria is necessary too.

Furthermore, we acknowledge the requirement to understand the switching between controls in the point stabilization examples. There is an element of sliding mode control to this, which has been extensively studied in the past, but not investigated or applied in relation to this application.

Additionally, a case for the need to investigate the optimality of the proposed scheme. This analysis could yield interesting results since we are dealing with steering the vehicle to the minima of some virtual potential function.

Finally, investigating this control design strategy on the kinematic car (or bicycle) is the next progression, as vehicles modelled this way are slated to take over the world.

Bibliography

- [1] A. D. Ames, X Xu, J. W. Grizzle, and P. Tabuada. Control barrier function based quadratic programs for safety critical systems. *IEEE Transactions on Automatic Control*, 62(8):3861–3876, 2016.
- [2] A. M. Bloch, P. S. Krishnaprasad, J. E. Marsden, and R. M. Murray. Nonholonomic mechanical systems with symmetry. *Archive for Rational Mechanics and Analysis*, 136(1):21–99, Dec 1996.
- [3] A. M. Bloch, J. E. Marsden, and D. V. Zenkov. Nonholonomic dynamics. *Not. AMS*, 52(3):320–329, 2005.
- [4] P Braun and C. M. Kellett. On (the existence of) control lyapunov barrier functions. *Preprint*, <https://eref.uni-bayreuth.de/40899>, 2018.
- [5] F. Bullo, N. E. Leonard, and A. D. Lewis. Controllability and motion algorithms for underactuated lagrangian systems on lie groups. *IEEE Transactions on Automatic Control*, 45(8):1437–1454, Aug 2000.
- [6] Francesco Bullo and Andrew D. Lewis. *Geometric Control of Mechanical Systems*, volume 49 of *Texts in Applied Mathematics*. Springer Verlag, New York-Heidelberg-Berlin, 2004.

- [7] J. Cortés, S. Martínez, J. P. Ostrowski, and H. Zhang. Simple mechanical control systems with constraints and symmetry. *SIAM J. Control and Optimization*, 41:851–874, 2002.
- [8] S. D. Kelly and R. M. Murray. Geometric phases and robotic locomotion. *Journal of Robotic Systems*, 12, 06 1995.
- [9] R. M. Murray, S. S. Sastry, and L. Zexiang. *A Mathematical Introduction to Robotic Manipulation*. CRC Press, Inc., Boca Raton, FL, USA, 1st edition, 1994.
- [10] T. Ohsawa. Geometric kinematic control of a spherical rolling robot. *arXiv preprint arXiv:1808.10106*, 2018.
- [11] D. Panagou. A distributed feedback motion planning protocol for multiple unicycle agents of different classes. *IEEE Transactions on Automatic Control*, 62(3):1178–1193, March 2017.
- [12] D. Panagou, H. G. Tanner, and K. J. Kyriakopoulos. Control of nonholonomic systems using reference vector fields. In *2011 50th IEEE Conference on Decision and Control and European Control Conference*, pages 2831–2836, Dec 2011.
- [13] D. Panagou, H. G. Tanner, and K. J. Kyriakopoulos. Control of nonholonomic systems using reference vector fields. In *2011 50th IEEE Conference on Decision and Control and European Control Conference*, pages 2831–2836, Dec 2011.
- [14] E. J. Rossetter, J. P. Switkes, and J. C. Gerdes. A gentle nudge towards safety: experimental validation of the potential field driver assistance system. In *Proceedings of the 2003 American Control Conference, 2003.*, volume 5, pages 3744–3749 vol.5, June 2003.
- [15] T Streubel. *Artificial Potential Fields as a Concept of Environment Modeling for Forward Directed Driver Assistance Systems*. PhD thesis, 10 2011.
- [16] S. D. Yang. Linearization and stability of nonholonomic mechanical systems. Master’s thesis, Queen’s University, 99 University Ave, Kingston, ON K7L 3N6, Canada, 2015.
- [17] D Zenkov, A. M. Bloch, and J. E. Marsden. Stabilization of the unicycle with rider. In *Proceedings of the IEEE Conference on Decision and Control*, volume 4, pages 3470 – 3471, 1999.